

8-2016

Microwave Plasma Surface Modifications of Carbon Fibers

Laura Ashley Smith

Clemson University, as6@g.clemson.edu

Follow this and additional works at: https://tigerprints.clemson.edu/all_theses

Recommended Citation

Smith, Laura Ashley, "Microwave Plasma Surface Modifications of Carbon Fibers" (2016). *All Theses*. 2438.
https://tigerprints.clemson.edu/all_theses/2438

This Thesis is brought to you for free and open access by the Theses at TigerPrints. It has been accepted for inclusion in All Theses by an authorized administrator of TigerPrints. For more information, please contact kokeefe@clemson.edu.

MICROWAVE PLASMA SURFACE MODIFICATIONS OF CARBON FIBERS

A Thesis
Presented to
the Graduate School of
Clemson University

In Partial Fulfillment
of the Requirements for the Degree
Master of Engineering
Materials Science and Engineering

by
Laura Ashley Smith
August 2016

Accepted by:
Dr. Marek Urban, Committee Chair
Dr. Philip Brown
Dr. Igor Luzinov

ABSTRACT

Fiber-polymer matrix interfaces are critical components of high performance composite materials. In this thesis we utilized microwave plasma surface reactions in the presence of maleic anhydride to functionalize carbon fiber surfaces. As a result, carboxylic acid and hydroxyl groups were generated, which facilitated covalent bonding to epoxy-based polymer matrices. Raman and attenuated total reflectance-Fourier transform infrared (ATR-FTIR) spectroscopy were utilized to characterize the fiber surfaces, whereas mechanical properties of newly formed interfaces were assessed using shear stress analysis. These studies show that using solventless microwave plasma surface modifications, interfacial mechanical properties of carbon fiber-epoxy matrix can be enhanced by $\sim 6\%$. The broader impact of these studies is that microwave plasma fiber surface modifications can be utilized to functionalize other polymeric and inorganic fibers, with an ultimate goal of enhancing composite interfacial and overall properties.

DEDICATION

I wanted to dedicate this to my parents, John and Corazon, for all of their support and love during my pursuit of a Master's Degree at Clemson University. And to my fiancé, Robert; he has motivated me greatly with his encouragement and devotion.

ACKNOWLEDGMENTS

I wanted to thank my advisor, Professor Urban, for helping me pursue a Master's Degree in Material Science and Engineering. Thank you for helping me find this path that will lead to many great adventures in the future. Thank you for helping me become a better researcher and a better writer. I also wanted to thank my committee members, Professor Brown and Professor Luzinov.

I wanted to give special thanks to Paul Rowland for his help in constructing the microwave plasma system that was used in this thesis.

I wanted to thank the Urban Research Group, Chris Hornat, Ying Yang, Dmitriy Davydovich, and Lauren Repp. Thank you for your help and support for the time I have been a part of the group. You guys have a great future ahead of you.

TABLE OF CONTENTS

	Page
TITLE PAGE	i
ABSTRACT.....	ii
DEDICATION.....	iv
ACKNOWLEDGMENTS	v
LIST OF TABLES.....	viii
LIST OF FIGURES	ix
 CHAPTER	
I. CHAPTER ONE: INTRODUCTION.....	1
1.1 CARBON FIBER PRODUCTION.....	2
1.2 ORDER AND DISORDER IN CARBON-BASED LATTICE STRUCTURES.....	7
1.3 INTERFACIAL INTERACTIONS BETWEEN CARBON FIBER SURFACES AND MATRIX	12
1.3.1 Wet chemistry surface reactions	13
1.3.2 Electrochemical surface reactions.....	15
1.3.3 Plasma surface reactions	16
1.4 MICROWAVE PLASMA MODIFICATIONS.....	18
1.5 SUMMARY	24
REFERENCES	27
 II. CHAPTER TWO: RESEARCH OBJECTIVE.....	 32
 III. CHAPTER THREE: RESEARCH METHODOLOGY	 35
3.1 MATERIALS.....	35
3.2 DESIGN OF MICROWAVE PLASMA SYSTEM.....	35
3.3 SURFACE MODIFICATION OF CARBON FIBERS.....	37

Table of Contents (Continued)

	Page
3.4 ANALYTICAL METHODS	38
3.4.1 Attenuated Total Reflectance-Fourier Transform Infrared Spectroscopy (ATR-FTIR).....	38
3.4.2 Raman Spectroscopy.....	38
3.4.3 Microbond Technique.....	39
REFERENCES	42
IV. CHAPTER FOUR: RESULTS AND DISCUSSION	43
4.1 CHEMICAL ANALYSIS OF SURFACE MODIFIED CARBON FIBERS.....	44
4.1.1 Raman spectroscopy analysis of MPMA and MPAr reactions	44
4.1.2 ATR-FTIR spectroscopy analysis of MPMA and MPAr reactions	47
4.1.3 Proposed mechanism for MPMA and MPAr surface modifications.....	54
4.2 MECHANICAL ANALYSIS OF FIBER-MATRIX INTERFACES	57
4.3 CORRELATION OF SPECTROSCOPIC AND MECHANICAL ANALYSIS	60
4.4 SUMMARY AND CORRELATION TO COMPOSITE MECHANICAL PROPERTIES	62
4.5 SUMMARY AND FUTURE WORK	66
REFERENCES	67
V. CHAPTER FIVE: Conclusion	69

LIST OF TABLES

Table	Page
1.1 Advantages and disadvantages of wet chemistry reactions	14
1.2 Advantages and disadvantages of electrochemical reactions	16
1.3 Summary of advantages and disadvantages of plasma surface treatment.....	18
1.4 Microwave plasma comparison to RF plasma	24
4.1 Area of D and G bands for PAN-based, MPMA, and MPAr	47
4.2 Interfacial shear stress values from microbond technique	59
4.3 Summary of interfacial shear stress values and I_D/I_G ratio	61
4.4 Estimations of critical length and composite tensile strength.....	65
4.5 Summary shear stress and estimated composite tensile strength values	65

LIST OF FIGURES

Figure	Page
1.1 Chemical structure of a carbon fiber surface.....	3
1.2 Production process for PAN derived carbon fibers	4
1.3 Dry-jet wet spinning process of PAN derived fibers	4
1.4 Polyacrylonitrile undergoing stabilization cyclization and oxidization.....	5
1.5 PAN derived fibers stabilized through oxidation process.....	6
1.6 Carbonization process for PAN derived carbon fibers	7
1.7 Schematic representation of an ideal graphite crystal lattice structure.....	8
1.8 Schematic of a diamond crystal lattice	9
1.9 Raman spectroscopy of I_D/I_G analysis of carbon fibers derived from different pre-cursor materials.....	11
1.10 Turbostatic crystal lattice structure of PAN derived carbon fibers.....	11
1.11 Proposed mechanism for surface functionalization by nitric acidic.....	14
1.12 Proposed mechanism for surface modification by aryl diazonium salts.	15
1.13 Possible mechanisms for generating functional groups through oxygen microwave plasma of carbon nanotubes.....	17
1.14 Plasma reaction that will modify the substrate surface through charged particle interactions.....	19
1.15 Microwave plasma surface modification of polytetrafluoroethylene for biomedical anti-microbial applications.....	23

List of Figures (Continued)

Figure	Page
2.1 Hydroxyl groups from a modified carbon fiber surface reacting with an epoxy group to form chemical bonds.....	32
3.1 Schematic diagram of the microwave oven plasma system	36
3.2 Schematic diagram of reaction chamber during MPMA reaction	37
3.3 Schematic diagram of the microbond set up for single fiber pull out	39
3.4 Epoxy bead on a single fiber prepared for testing	40
3.5 Schematic diagram of microbond single fiber experiment	41
4.1 Schematic diagram of sp^2 to sp^3 carbon fiber surfaces hybridization	44
4.2 Raman spectra curve fitting was utilized to determine I_D to I_G ratios of (a) PAN-based, (b) MPMA, and (c) MPAr fibers	46
4.3 ATR-FTIR spectra of MPMA carbon fibers in the (a) $3800-2600\text{ cm}^{-1}$ (b) $1750-1600\text{ cm}^{-1}$ and (c) $1340-1200\text{ cm}^{-1}$ regions.....	48
4.4 ATR-FTIR spectra of MPAr fibers in the (a) $4000-2600\text{ cm}^{-1}$ (b) $1750-1600\text{ cm}^{-1}$ and (c) $1350-1200\text{ cm}^{-1}$ regions.....	50
4.5 CH_2 bending region of PAN-based, MPAr, and MPMA fibers.....	52
4.6 MPMA reactions to carbon fiber surfaces	53
4.7 Proposed mechanism for MPMA attachment to carbon fiber surfaces	56

List of Figures (Continued)

Figure	Page
4.8 (a) MPMA and (b) MPAR reactions with epoxy groups leading to enhancement of interfacial interactions between the fiber and the matrix	57
4.9 Microbond images (a) epoxy microbead (l_m) (b) fiber diameter (d)	58
4.10 I_D/I_G ratios plotted as a function versus interfacial shear stress (MPa) for PAN-based, MPMA, and MPAr	61
4.11 Schematic diagram of interfacial interfaces of (a) unmodified and (b) surface modified carbon fiber surfaces	63
4.12 Estimated composite tensile strength (GPa) plotted as a function versus interfacial shear stress (MPa) (a) failure at the interface and (b) failure in the fiber for PAN-based, MPMA, and MPAr	66

CHAPTER ONE

INTRODUCTION

High performance composite materials emerged during the 1960s for aerospace applications. They were developed to replace construction materials which were traditionally used in industrial applications.¹ Prior to the emergence of high performance composites, aluminum (Al) was the prevailing structural component in aerospace applications; however, Al's performance and cost came into question as the aerospace industry expanded. Al is affected by corrosion, due to chemical and electrochemical processes; for example, water vapor that contains salt can corrode an aircraft by creating pits and etches the surface of the metal, weakening the structure.² The criteria for developing new materials were high strength, stiffness, toughness, and light weightness.¹ High performance composite materials meet these criteria, which could be further tailored for specific applications.

High performance composite materials are composed of two distinct components: the reinforcement material and the matrix material. Both of these distinct components create a material that has enhanced material properties that has a mixture of characteristics from both of the components. The most common reinforcement materials that are utilized in composites are carbon, polyparaphenylene terephthalamide (aramid), boron, and glass fibers. Thermoset matrices that are typically utilized in composites are epoxy, polyester, vinyl ester, and phenol-formaldehyde based polymers.³ These components, the reinforcement material, and the matrix, define the composite's usage and

limitations in many applications. Because carbon fiber reinforced plastics exhibit many desirable properties, they gained tread as a material component that could be used as a replacement over certain metal materials. Aircraft chassis, automotive frames, boat hulls, and military applications provided a variety of ways for carbon fiber reinforced plastics to be used instead of Al, wood, copper, and steel construction materials.⁴ This expansion into a variety of applications fueled the development of new composites and manufacturing processes of the individual components, manufacturing methods to produce a composite, as well as interfacial studies between the reinforcement and the matrix material. Also destructive and non-destructive testing methods were developed. The focus of this thesis is to design, develop, and understand the role of interfaces between the fiber and the matrix components ultimately leading to improved mechanical properties.

1.1 CARBON FIBER PRODUCTION

Carbon fibers have been used in a variety of composite materials because of their beneficial chemical properties such as corrosion resistance, chemical stability, high thermal conductivity and low electrical resistivity¹, as well as physical properties including low density, high strength and high stiffness.¹ Carbon fibers are made of conjugated aromatic rings that are cross-linked together to form a crystal lattice structure; this chemical structure is illustrated in Figure 1.1. Based on processing and the type of pre-cursors that they were produced from, they can impact the carbon fibers greatly. The pre-cursors affect the carbon fibers' unique characteristics and structural differences,

causing a change in mechanical properties that allows them to be used in specific applications.

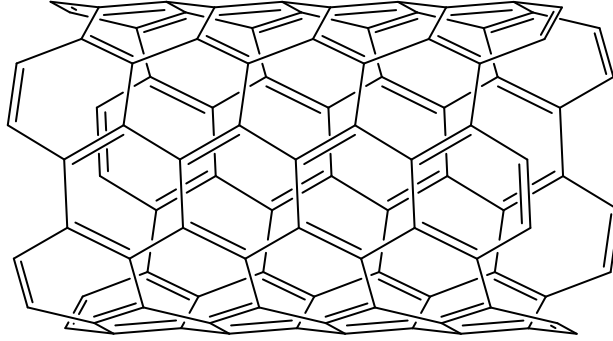


Figure 1.1: Chemical structure of a carbon fiber surface.

In processing carbon fibers, the pre-cursor material must fulfill three criteria⁵:

1. It has to be spun into a fiber
2. It cannot melt
3. The fiber has to be stabilized before undergoing carbonization

From these criteria, there are three main pre-cursors that are commercially used in processing carbon fibers, which are:

- Polyacrylonitrile-based (PAN derived)
- Pitch-based
- Rayon-based

PAN derived carbon fibers are commonly utilized in many applications because they possessed better mechanical properties compared to other pre-cursors. Figure 1.2 illustrates the production process of PAN derived carbon fibers from the beginning steps of polymerizing PAN, fiber spinning, oxidation, and carbonization.⁶

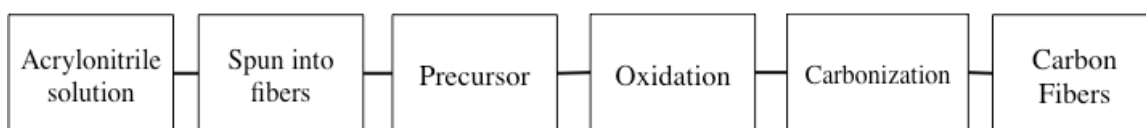


Figure 1.2: Production process for PAN derived carbon fibers.⁶

PAN derived fibers are polymerized by solution polymerization, bulk polymerization, emulsion polymerization, or aqueous dispersion polymerization.⁶ The polymerization involves primarily acrylonitrile monomer, but 5% of a co-monomer is added to improve the crystal structure and to help stabilize the fiber. One example of the monomers that have been utilized is acrylic acid.⁵ The PAN polymer solution is spun into fiber by three methods: wet spinning, dry-jet wet spinning, and dry spinning. Dry-jet wet spinning grew in popularity because it produced better overall mechanical properties.^{4,5} Dry-jet wet process spinning is schematically shown in Figure 1.3.

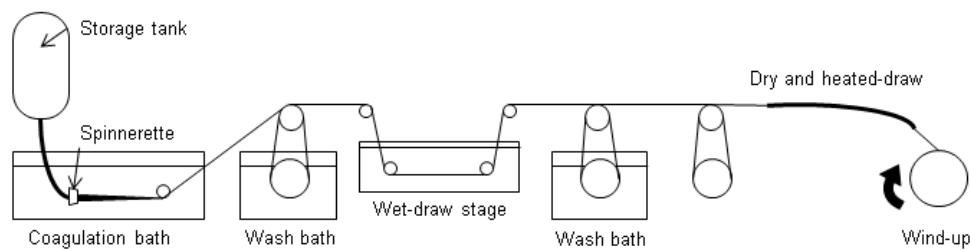


Figure 1.3: Dry-jet wet spinning process of PAN derived fibers.⁷

As shown, the polymer solution is extruded into a coagulation bath, and pulled under tension into the wash bath, wet-draw stage, secondary wash bath, and drying stage. Fibers are held under tension during this process to maintain molecular orientation throughout the fiber. The tension speed for each stage shown in Figure 1.3 is being pulled faster than the previous to keep drawing out the orientation which will that improve the overall mechanical properties. The next step is to stabilize the fibers, which is achieved by

converting the linear chains to cyclic chains by thermal oxidation and cyclization to form the hexagonal rings.⁸ This is shown in Figure 1.4. The role of oxygen present during the stabilization process was not fully understood, so there were studies performed to understand its role. It was concluded that the role of oxygen is to assist in the cyclization process by creating reaction sites and the oxygen groups were used in crosslinking during the carbonization process.⁹

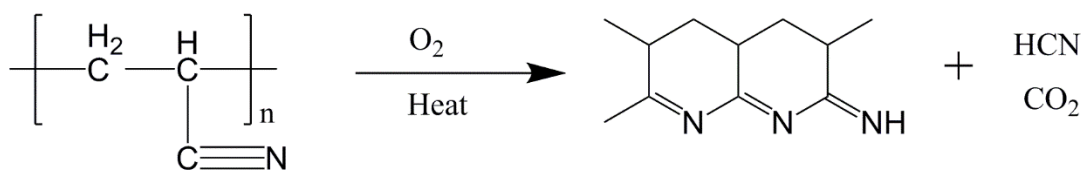


Figure 1.4: Polyacrylonitrile undergoing stabilization cyclization and oxidation.⁸

Figure 1.5 shows the stabilization process where the fibers are pulled under tension through the oxidation oven that contained heated circulated air and wound into spools for the next process.

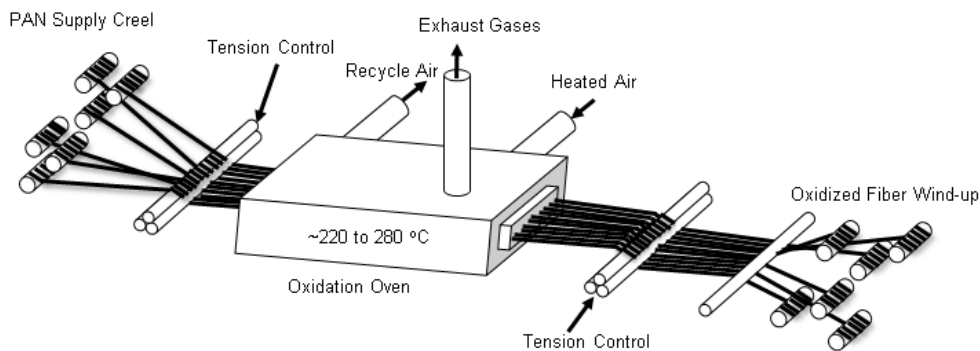


Figure 1.5: PAN derived fibers stabilized through oxidation process.⁷

The next step of the process is to carbonize the fibers by utilizing the hydrogen, nitrogen, and oxygen atoms that are still present in the cyclic rings and crosslinks the chains

together. The carbonization phase is shown schematically in Figure 1.6 and consists of two processes: dehydrogenation (A) and denitrogenation (B). The carbonization processing steps are operated under an inert gas to prevent any side reactions from occurring to keep final product as pure as possible. Dehydrogenation (A) is achieved at a temperature range of 400-600 °C, where the hydrogen atoms diffuse out of the two cyclized chains as they crosslink. After dehydrogenation, the temperature is increased up to 1,500 °C to start the denitrogenation (B) process. The nitrogen atoms diffuse out as the system and crosslinking of fiber continues. After carbonization step, the fibers can be heated up further to 3,000 °C to heat treat the growing the crystals within the structure to produce graphite fibers.⁵

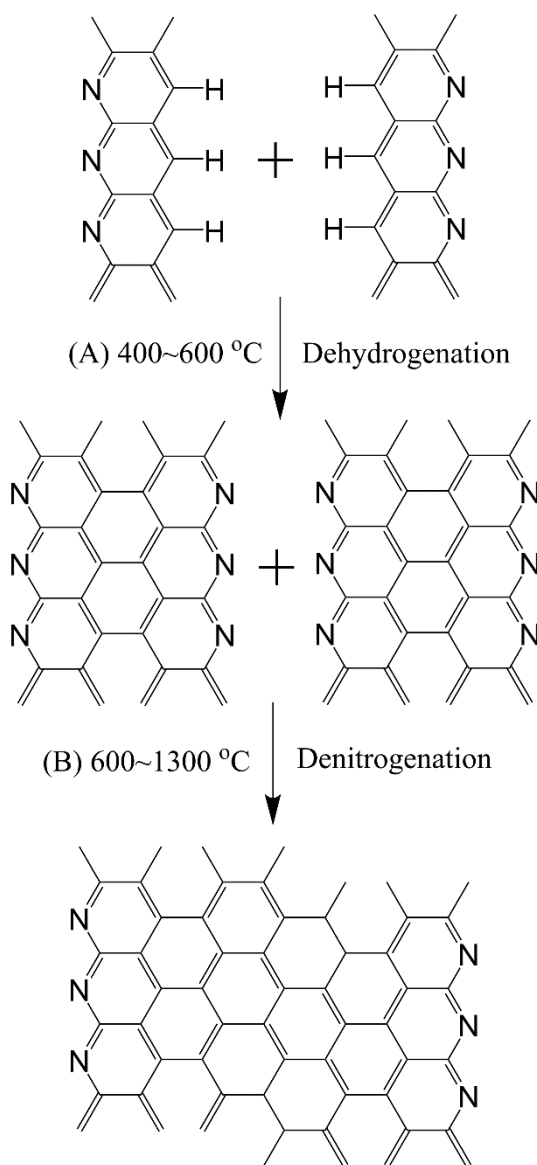


Figure 1.6: Carbonization process for PAN derived carbon fibers.⁸

1.2 ORDER AND DISORDER IN CARBON-BASED LATTICE STRUCTURES

Crystal lattice structures are essential in describing how different planes of atoms will interact with each other and affect their chemical and mechanical properties. These structures also describe the symmetry and how different planes of atoms will interact utilizing a unit cell for interpretation. This unit cell observes how the atoms are arranged

in either two-dimensional or three-dimensional lattice types.¹⁰ In an effort to understand how carbon atoms are arranged, three-dimensional lattice types will be considered in analyzing graphitic and amorphous carbon structures. Graphitic carbon has a crystal lattice that resembles a hexagonal close-packed structure, which is illustrated in Figure 1.7. The carbon planes have alternating layers of ABA, which causes the planes to have a high atomic packing factor. This causes it to achieve a high degree of order within the structure.

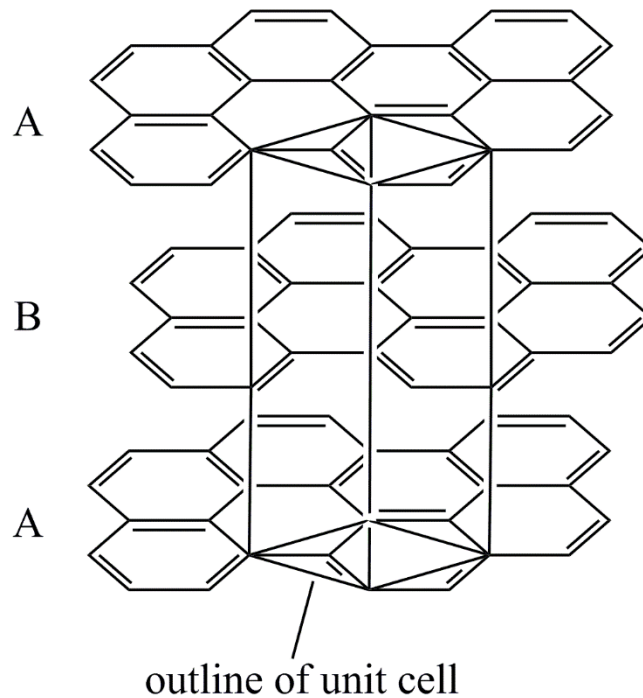


Figure 1.7: Schematic representation of an ideal graphite crystal lattice structure.¹¹

An amorphous carbon crystal lattice has a diamond structure, which is illustrated in Figure 1.8. This structure shows a low atomic packing factor compared to the graphitic crystal lattice. In carbon fibers, these crystal structures are heavily dependent on the type

of pre-cursor utilized in the manufacturing of the carbon fibers, and this is critical in observing the changes to the surface of the material.

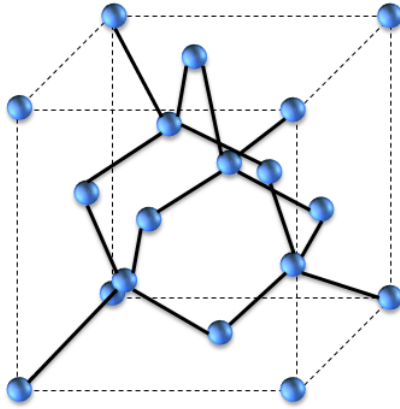


Figure 1.8: Schematic of a diamond crystal lattice.¹⁰

Crystal lattice structures do not provide all the information necessary to understand surfaces of carbon materials, especially in carbon fiber surfaces. Hybridization theory can describe crystal lattice structures from the perspective of bonds between atoms. In hybridization theory, different hybrid types, such as sp , sp^2 , and sp^3 , affect the atomic orbital conformations. This affects how they interact with other atoms or with a plane of atoms. sp^2 and sp^3 hybridizations are important for carbon materials because they reflect graphitic and amorphous crystal lattice structures. sp^2 hybridization corresponds to having three sigma bonds and one pi bond between atoms, which would result in a planar conformation. sp^3 hybridization corresponds to having four sigma bonds between atoms, which would result in a tetrahedral conformation.¹² Raman spectroscopy is used to analyze the surface because it is sensitive to hybridization changes in carbon materials.¹³ Since carbon materials are comprised of conjugated aromatic rings, Raman spectroscopy exhibits two distinct characteristic bands. The G-band, “graphite” band¹⁴, appears

approximately at 1580 cm^{-1} . The D-band, described as “disordered”¹⁴ band, appears approximately at $1330\text{-}1350\text{ cm}^{-1}$.^{13,14,15} These bands are important because they directly correlate to the crystal lattice and hybridization present on the carbon surfaces. The G-band indicates that there is sp^2 hybridization present which correlates to the presence of a highly ordered structure (hexagonal close-packed structure). The D-band indicates that there is sp^3 hybridization present which correlates to an amorphous structure (diamond crystal lattice). Raman spectroscopy is used to analyze carbon material, which between the areas under G and D bands using deconvolution, the intensity of D-band (I_D) over the intensity of G-band (I_G) into a ratio that can allow us to differentiate whether the material is dominated by either graphitic or amorphous structures.¹⁴

The distinction between graphitic and amorphous structures are critical when analyzing carbon fiber surfaces because both bands are sensitive to surface changes and on the type of pre-cursor that was initially used. Figure 1.9 shows how the pre-cursor material changes the I_D/I_G ratio in Raman spectroscopy. Pitch-based carbon fiber will have a lower I_D/I_G because it has an ideal graphitic structure that dominates its morphology, while PAN derived carbon fibers will have a higher I_D/I_G . This is due to PAN derived carbon fibers undergoing cyclization to achieve aromatic rings that are further cross-linked by the carbonization and graphitization process. During these processes, defects can be introduced into the structure that prevents the plane of aromatic rings from becoming stacked on top of each other into the hexagonal close-packed lattice. As a result, the structure of a PAN derived carbon is shown in Figure 1.10 that visually represents how the carbon planes are disordered (I_D) but still maintains a degree of order

to them (I_G). The PAN derived carbon fibers are classified as being turbostatic due to the higher spacing between the planes.

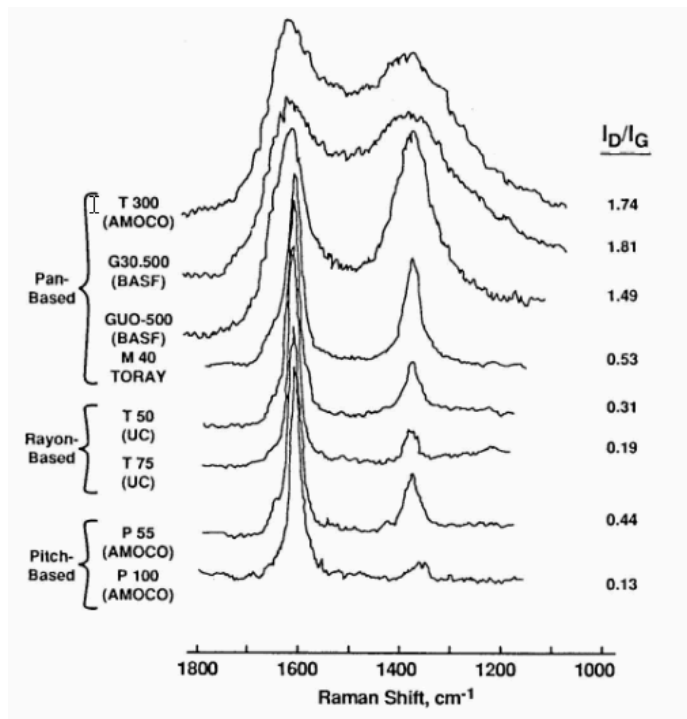


Figure 1.9: Raman spectroscopy of I_D/I_G analysis of carbon fibers derived from different pre-cursor materials.¹⁶

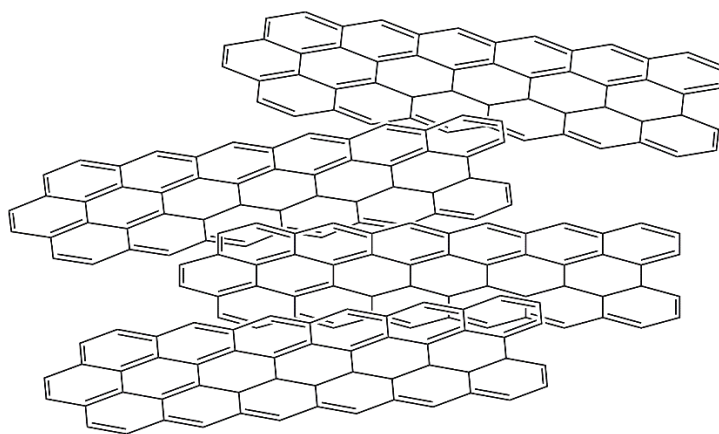


Figure 1.10: Turbostatic crystal lattice structure of PAN derived carbon fibers.¹¹

Raman spectroscopy is a critical analytical tool in distinguishing the characteristic bands and quantifying the I_D/I_G ratio. This is critical in analyzing the surface of the carbon fibers as it undergoes surface alteration thus resulting in hybridization changes which will be further discussed in the upcoming chapters.

1.3 INTERFACIAL INTERACTIONS BETWEEN CARBON FIBER SURFACES AND MATRIX

In high performance composites the interfacial interactions between reinforcement fiber surface and matrix material are critical because poor adhesion between the binder (polymer matrix) and the fiber may result in catastrophic failure of a composite. Especially in carbon fiber reinforced plastics, where the carbon fiber surface is inert, so it is harder to achieve a strong and desirable adhesion. This inert surface is due to the graphitization process of carbon fibers because there is a change in the surface morphology, which results in no functional groups being present on the surface.¹⁶ Thus, understanding the interfacial behavior between the surface fiber and matrix is critical to mechanical properties. The interactions will dictate how much load can be transferred from the fiber to the matrix material under stress. If the fibers are being pulled away from the matrix as a result of shear occurring within the matrix, the load is unable to be transferred into the matrix, which results in pre-mature failure in a composite.¹⁸ To enhance the adhesion between the fiber and the matrix interface, the inert fiber surfaces have to be modified by chemical or physical means. Surface modifications may be physical and chemical nature, and should only affect the properties of the surface, but not the bulk of the material.¹⁹ Chemical surface modification are the primary method used to

alter carbon fiber surfaces. Upon surface modification, the presence of surface functional groups will determine the strength of the fiber-matrix interactions. Several types of surface modifications have been developed, such as, oxidation, reduction, grafting, cross-linking, etching, and deposition. For carbon fibers, the methods for chemical surface modifications are classified as:

- Wet chemistry reactions
- Electrochemical reactions
- Plasma reactions

1.3.1 Wet chemistry surface reactions

Wet chemistry modifications rely on the utilization of acid oxidation to generate oxygen containing functional groups onto the carbon fiber surfaces. Oxidation chemistry is well understood and requires the use of highly acid or basic chemicals, which can be commercial obtained. So it can be considered a conventional technique for modification. An example of wet chemistry surface modifications is to utilize nitric acid to oxidize the surface and form carboxyl and phenolic group, as shown in Figure 1.11.²⁰ Typically, the carbon fibers are treated in a solution of 70% nitric acid, at an elevated temperature of 115 °C. After treatment, the carbon fibers are washed to remove excess amounts of nitric acid and dried before being further reacted.²⁰

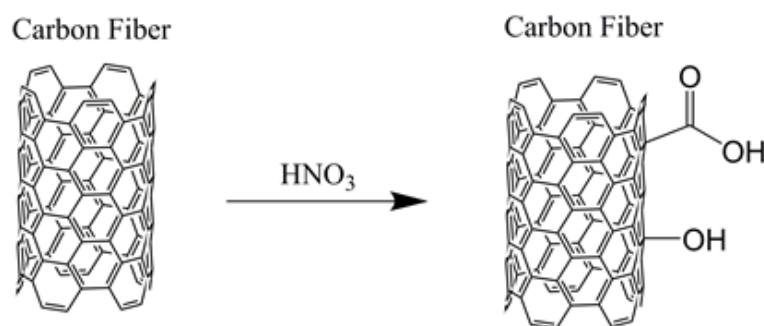


Figure 1.11: Proposed mechanism for surface functionalization by nitric acidic.²⁰

Another technique used to generate functional groups is to graft a monomer onto the carbon fiber surface. For example, maleic anhydride monomer reacted with carbon fibers in a solution of methyl cyclohexane at 101 °C to generate the carboxyl and phenolic groups.²¹ Wet chemistry reactions are conventional techniques that have advantages and disadvantages which are summarized in Table 1.1.²² Wet chemistry has the advantages of using a strong acid or base for the reaction to occur and oxidation chemistry relies on the generation of polar groups being formed. The process for using this technique can be adjusted for either batch or continuous processes. However, the material can be damaged if the oxidation process goes for extended amounts of time and generates large amount of waste. In order for the functionalization to be generated on the surfaces.

Table 1.1: Advantages and disadvantages of wet chemistry reactions.²²

Advantage	Disadvantage
<ul style="list-style-type: none"> • Simple reactions • Process can be run as batch or continuous 	<ul style="list-style-type: none"> • Can affect bulk properties • Large volume of hazardous waste generated • High temperature reactions

1.3.2 Electrochemical surface reactions

In electrochemistry, the system is comprised of three main components:

- Cathode
- Anode
- Electrolyte solution

In electrochemical surface modifications, the carbon fibers would act as the anode, the cathode would be a metal (e.g., stainless steel), and the electrolyte solution would vary depending on the design of the experiment. Electrochemical modifications have been studied to understand its effects on altering the chemical nature and morphology of carbon fiber surfaces.²³ Interactions between the electrolyte solution with the carbon fiber surfaces have also been examined. An example of this would be analyzing how aryl diazonium salts generate functional groups through electrochemical reductions. Which were further analyzed by studying how the aryl diazonium salt modified carbon fiber would interact with an epoxy matrix.²⁴

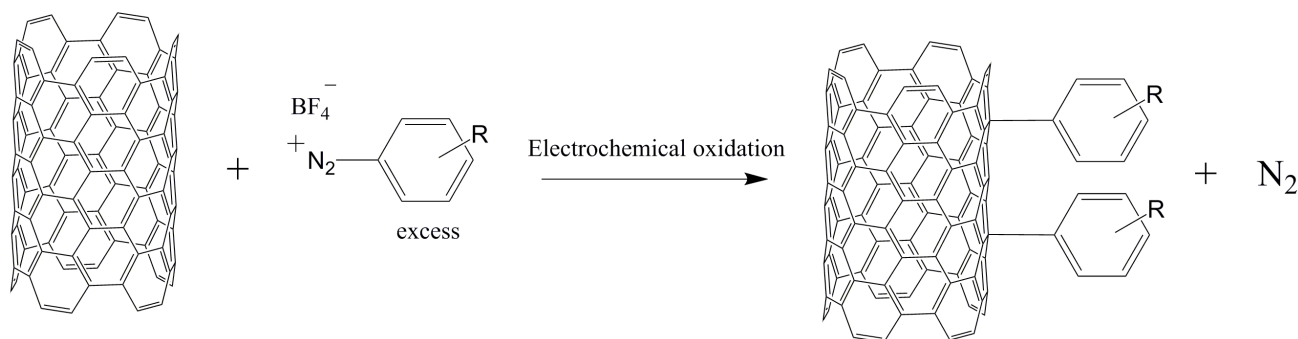


Figure 1.12: Proposed mechanism for surface modification by aryl diazonium salts.²⁴

The advantages and disadvantages of using electrochemical reactions as a surface treatment are summarized in Table 1.2.²⁵ These reactions can be used to process fibers in a batch or continuous process and the equipment mostly involves the use of a cathode, anode, and reaction solution. This reaction creates stable covalent bonds to the modified surface and is a reproducible process that can be used repeatedly.

Table 1.2: Advantages and disadvantages of electrochemical reactions.²⁵

Advantage	Disadvantage
<ul style="list-style-type: none"> • Bulk properties are unaffected • Reagents are inexpensive • Utilizes basic electrochemical equipment (reaction chamber, cathode, anode, and reaction solution) • Reproducible • Modified surface is chemically stable • Resistant to harsh environmental effects 	<ul style="list-style-type: none"> • Large volume of hazardous waste generated • Difficult to achieve multilayers on the surface • Reaction with carbon fiber surface is not fully understood

1.3.3 Plasma surface reactions

Plasma is a viable technique that can be used to alter the surface of a material's chemical and physical properties; however, plasmas can be created differently and depend on the voltage source utilized to excite the carrier gas. In order to generate plasma, a voltage source such as AC, DC, RF, or microwave, is utilized. A surface treatment for fiber surface modifications utilizes oxygen plasma treatment by direct current plasma. Oxygen plasma treatments have been observed to etch the surface of the material and generate functional groups. One study showed that oxygen plasma treatments improved interfacial shear of different fibers, such as, poly (1,4-phenylene-cis-benzobisoxazole), Kevlar, and carbon, depending on the amount of time that the surface

was exposed to the plasma treatment.²⁶ Another plasma surface modification utilized oxygen plasma treatment by microwave plasma on carbon nanotubes.

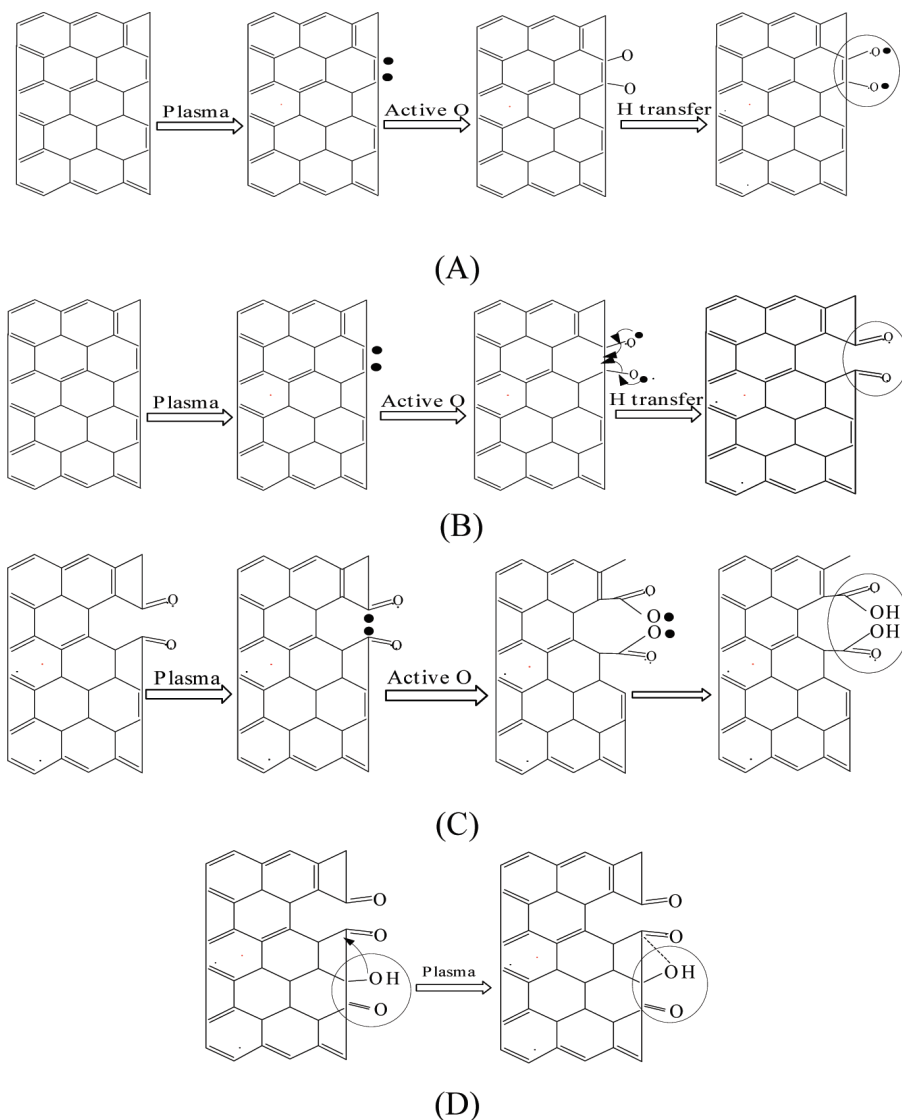


Figure 1.13: Possible mechanisms for generating functional groups through oxygen microwave plasma of carbon nanotubes.²⁷

Figure 1.13 illustrates how microwave plasma was utilized to modify the surface of carbon nanotubes with plasma. The plasma was produced with oxygen, which interacted with the surface to generate polar groups, such as alcohol, carboxylic acid, ester, and

ether groups. These functional groups enabled the carbon nanotubes to be further reacted with other molecules.²⁷ This shows that plasma surface modifications is a viable technique used to generate functional groups at the interface. There are advantages and disadvantages of plasma surface treatments in industrial usage compared to conventional techniques summarized in Table 1.3.²²

Table 1.3: Summary of advantages and disadvantages of plasma surface treatment.²²

Advantages	Disadvantages
<ul style="list-style-type: none"> • Does not affect bulk properties • Process can run either batch or continuous • Small waste generation • Reduction in chemical usage • Applied to a variety of applications 	<ul style="list-style-type: none"> • Requires trained personnel • Reactions are heavily dependent on the equipment and reaction conditions • Complex reaction schemes

Section 1.4 discusses more detail about plasma and microwave plasma surface modifications.

1.4 MICROWAVE PLASMA MODIFICATIONS

With regard to this research, microwave plasma surface modifications is utilized and studied to observe surface alterations on carbon fiber surfaces. This section is used to provide background information about plasma, plasma reactions, and compare microwave plasma to traditional RF plasma. Neutral gases are converted into plasma with either high temperature or high voltage that unbinds positive and negative particles. This breaking down of neutral gas into positive, negative, and neutral ions allows for the creation of ionized gas, illustrated in Figure 1.14.

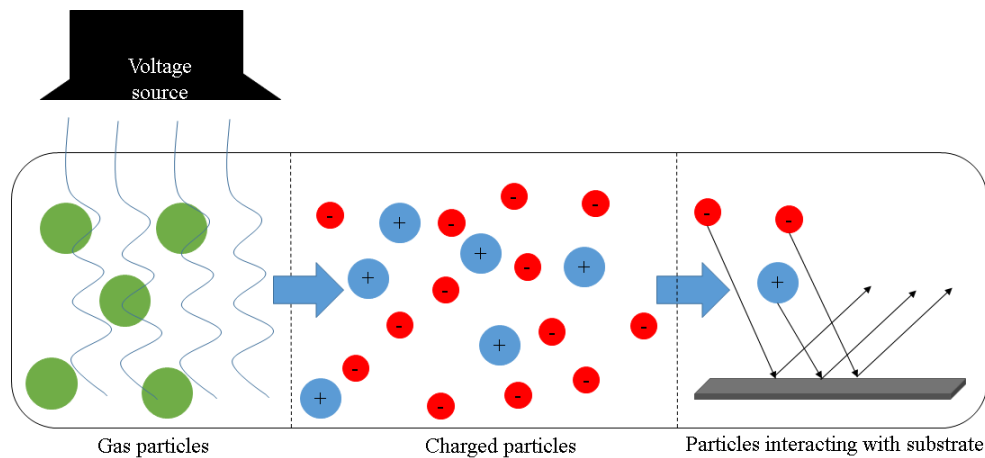


Figure 1.14: Plasma reaction that will modify the substrate surface through charged particle interactions.

As these charged particles interact, they give off energy and photons that emit plasma or a discharge glow. The amount of charged ions created during this breakdown depends on the following:

- Voltage source: AC, DC, radio frequency (RF), or microwave frequency
- Gas species, pressure, and flow rate
- Reactor geometry
- Distance utilized to ionize the gas

Within the plasma, the positive and negative particles still possess coulomb forces that act against each other. As the positive and negative particles within the plasma move about, they generate and respond to both electric and magnetic fields.²⁸ Also, as the charged particles collide against each other, they follow the law of conservation of energy, causing their energy and momentum to be transferred through collision reactions.

These collision reactions are categorized by three collision types that occur, they are as follows²⁸:

- Elastic collisions
- Inelastic collisions
- Super-elastic collisions

Elastic collisions occur when particles collide together and separate from each other towards different directions. This occurs because their momentum and total kinetic energy are transferred equally and no energy is lost during the transfer. Inelastic collisions occur when particles collide and stick closely together prior to separating upon impact with one another. The result of an inelastic collision causes the particles to lose momentum and total kinetic energy. Super-elastic collisions occur when particles collide together and separate with more energy. This occurs because there is a transfer of internal energy between the two particles that is redistributed. As these collisions occur, they can be used to alter a material's surface by transforming the energy of the collisions into chemical energy. This causes a reaction that will be exhibited as a change in physical and chemical properties. These collisions can be distinguished as three reaction types²⁸:

- Electron impact: ionization, dissociation, dissociative ionization, dissociative attachment, electronic excitation, rotational-vibrational excitement, and momentum transfer
- Neutral: dissociation, Penning ionization, atom transfer, rearrangement, recombination, energy transfer, relaxation, and momentum transfer

- Ion: neutralization, associative detachment, charged transfer, dissociative charge transfer, and momentum transfer

These reactions can also be described as having the kinetic energy, from the collisions, transformed into chemical energy that is used for plasma surface modifications or plasma polymerizations on different types of surfaces. Reactions are achieved by adsorption or desorption.²⁸ Adsorption is where particles are absorbed onto the surface of the material by chemical attractive forces. Desorption is the result of particles being released from the surface of the material.²⁸ These reactions are important for how polymer films are formed under plasma reactions. Plasma polymerizations form polymer films through adsorption and deposition with a surface present, so these films are achieved differently from the conventional polymers.²⁹ The monomers that are used to form these thin films are introduced into the system typically as organic gasses, such as methane, ethane, and propane. There are some monomers that are introduced into the system as a solid monomer and sublimated into their vapor phase. These films are achieved through free-radical polymerization.^{29, 30, 31} The free-radicals will initiate the process by interacting with a monomer molecule create a reactive species that continues to propagate the long chains until termination. There are some instances where crosslinking occurs during the propagating due to the presence of other particles during the reaction. These particles can collide into the polymer chain and create another reactive site that will continue to propagate until termination. It is described that termination in plasma polymerization is not typical; furthermore, there are two types of termination^{30, 29}:

- The propagating chains will terminate quickly so the film results in a low molecular weight and highly cross-linked system
- The propagating chains will terminate by rearranging themselves to have unsaturated end groups

Some examples of thin films generated by plasma polymerization are saturated and unsaturated hydrocarbons. They were studied originally to develop a mechanism that would explain how plasma was creating these films. The operating conditions for this study was to utilize monomer gases that were fed into a reaction chamber that held two parallel electrodes that were subjected to a RF generator, to produce the plasma.³¹ In another study, they utilized maleic anhydride monomer to produce films that would have increased adhesion to different substrates by RF plasma. They proposed a mechanism where the double bond carbon in the structure would be initiated by a free radical that would propagate and form the film. The reaction was stabilized by a resonance structure with the oxygen in the monomer.³² In addition to forming films by plasma polymerization, plasma can be used to alter the surface chemistry of a material by using the neutral gas.

In Section 1.3.3, it was discussed that plasma is a viable technique that can be used to alter the surface of a material's chemical and physical properties; however, all plasmas are created differently and depends on the voltage source used to excite the neutral gas. Microwave plasma is generated by using a microwave frequency of ~2.4 GHz as the voltage source instead of other sources such as RF, DC, and AC. The majority of microwave plasma reactions are held at low-pressure conditions, but can be

operated near atmospheric pressures. Furthermore, they do not utilize electrodes in the reaction chamber in order for the plasma to be generated; only the magnetron and waveguide is utilized. Microwave wave plasma has been utilized to generate functional groups on various substrates, for example, carbon fibers³³, carbon nanotubes²⁷, and polymer surfaces.

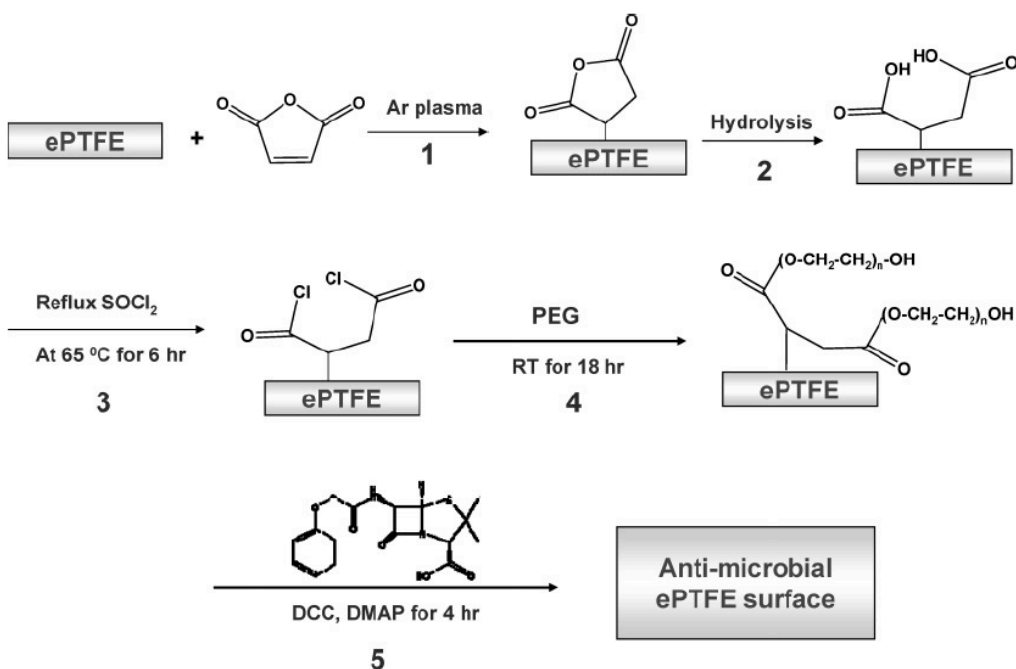


Figure 1.15: Microwave plasma surface modification of polytetrafluoroethylene for biomedical anti-microbial applications.³⁴

Figure 1.15 illustrates how microwave plasma was utilized to modify the surface of polytetrafluoroethylene with carboxylic acid groups to facilitate the attachment of penicillin groups in order to exhibit antibacterial functionality.³⁴ In many studies that involve plasma surface modifications, RF plasma is traditionally more utilized over microwave plasma. The disadvantage of using RF plasma is how the plasma is controlled

(i.e., the current and voltage produced can damage or destroy the substrate surface).

Utilization of a secondary set of electrodes and RF generator minimize this disadvantage.

Another difference is the frequency that is utilized to generate plasma. A RF generator has a frequency of ~13.56 MHz, while a microwave generator has a frequency of ~ 2.4 GHz. Table 1.4 summarizes the advantages and disadvantages of using microwave plasma compared to RF plasma surface modifications.³⁵

Table 1.4: Advantages and disadvantages of microwave plasma.³⁵

Advantages	Disadvantages
<ul style="list-style-type: none">• Solvent less system• No waste generation• Controllable reaction• Less consuming reaction times• Efficient reaction• No electrodes utilized in reaction• Promotes higher chemical reactivity• High degree of uniformity	<ul style="list-style-type: none">• Low pressure operating conditions• Scale-up of the process is challenging

Furthermore, microwave plasma has the advantage of removes a higher degree of contamination, generates higher amount of chemical functionalization, and deposits polymer film on substrate material.

1.5 SUMMARY

High performance composite materials were developed not only as an alternative to metal construction materials, but also obtain high strength-to-weight ratio, which has led to numerous applications. Since the strength-to-weight ratio is particularly important in aerospace applications, replacing Al was an obvious extension. From the development of high performance composite materials, carbon fiber reinforced plastics gained popularity due to their versatility. Specifically, high temperature resistance, low density,

and corrosion resistance make these materials attractive for many structural applications. For example, PAN-based carbon fiber reinforced plastics are used in the majority of structural components since they have higher strength than the other types of carbon fibers. Due to the inert surface of PAN derived carbon fibers, the matrix is unable to adhere well onto the fiber's surface. Consequently, surface modifications are necessary to enhance adhesion at the interface to minimize the possibility of catastrophic failure. There are three surface modifications that are utilized in carbon fiber surface modifications: wet chemistry modifications, electrochemical modifications, and plasma surface modifications. These surface modifications are used to generate functional groups that will improve the adhesion between the fiber surface and matrix by creating chemical covalent bonds. Out of the three surface modifications discussed, microwave plasma surface modifications are utilized to generate more chemical functional groups, are solvent free, and rapid compared to other surface modifications. The objective of this thesis is not only to utilize microwave plasma surface reactions in the presence of maleic anhydride to form reactive acid groups on the surface of carbon fibers, but also to understand molecular processes that govern these processes. The ultimate goal is create covalent bonds between the fibers and an epoxy matrix and quantitatively assess how chemical reactions will impact mechanical interfacial properties represented by the measurement of shear stress required to physically pull fibers out of the matrix.

The remaining parts of this thesis consist of four chapters. Chapter 2 focuses on the research objective, while Chapters 3, 4, and 5 discusses the methodology, results, and conclusion of the experiments conducted. Chapter 2 discusses and emphasizes the

importance of studying the interface between the fiber and the matrix, and how microwave plasma surface modifications will be utilized to enhance this relationship. Chapter 3 focuses on the analytical methods and operating conditions for the microwave plasma experiments. Chapter 4 discusses the surface characterization and mechanical results of how the interface was affected by the microwave plasma experiments and how the interfacial mechanical properties are utilized to predict the improvement in the composite tensile strength. Chapter 5 concludes the thesis by emphasizing the importance of surface modifications towards fiber-matrix interfacial relationship and the research was achieve this surface alteration through microwave plasma.

REFERENCES

1. Chawla, K.K., *Composite materials: Science and Engineering*. Springer Science & Business Media: New York, **2012**.
2. U.S. Department of Transportation: Federal Aviation Administration. Aviation Maintenance Technician Handbook – General.
http://www.faa.gov/regulations_policies/handbooks_manuals/aircraft/amt_handbook/
3. Bunsell, A.R.; Renard, J., *Fundamentals of fibre reinforced composite materials*. CRC Press: **2005**.
4. U.S. Department of Transportation: Federal Aviation Administration. Aviation Maintenance Technician Handbook-Airframe, Volume 1.
http://www.faa.gov/regulations_policies/handbooks_manuals/aircraft/amt_airframe_handbook/
5. Bahl, O.P.; Shen, Z.; Lavin, J.G.; Ross, R.A., *Manufacture of Carbon Fibers. Carbon fibers*; Peng, J.C.M.; Donnet, J.B.; Wang, T.K.; Rebouillat, S., Eds; Marcel Dekker: New York, **1998**, 3, 1.
6. Park, S.J.; Lee, S.Y. History and Structure of Carbon Fibers. *Carbon Fibers*; Park, S.J., Ed.; Springer Series in Materials Science, **2014**, 1.
7. Edie, D.D, The effect of processing on the structure and properties of carbon fiber. *Carbon* **1998**, 36(4), 345-362.
8. S.J. Park, S.J.; Heo, G.Y. Precursors and manufacturing of Carbon Fibers. *Carbon Fibers*; Park, S.J., Ed.; Springer Series in Materials Science, **2014**, 31.

9. Fitzer, E.; Muller, D.J. The influence of oxygen on the chemical reactions during stabilization of pan as carbon fiber precursor. *Carbon*, **1975**, 13(1), 63-69.
10. Kittle, C. *Introduction to solid state physics*. John Wiley & Sons: Hoboken, **2004**.
11. Pierson, H.O. *Handbook of carbon, graphite, diamond, and fullerenes properties, processing, and applications*. Noyes Publications: Park Ridge, **1993**.
12. Murry, J.E. *Organic Chemistry*. Brooks Cole: Boston, **2012**.
13. Knight, D.S.; White, W.B., Characterization of diamond films by Raman Spectroscopy. *Journal of Materials Research*, **1989**, 4(2), 385-393.
14. Jawhari, T.; Roid, A.; Casado, J., Raman spectroscopic characterization of some commercially available carbon black materials. *Carbon*, **1995**, 33(11), 1561-1565.
15. Tuinstra, F.; Koenig, J.L., Raman Spectrum of Graphite. *Journal of Chemical Physics*, **1970**, 53(3), 1126-1130.
16. Fitzer, E., Pan-based carbon fibers-present state and trend of the technology from the viewpoint of possibilities and limits to influence and to control the fiber properties by the process parameters. *Carbon*, **1989**, 27(5), 621-645.
17. Peng, J.C.M.; Donnet, J.B.; Wang, T.K.; Rebouillat, S. Surface Treatment of Carbon Fibers. *Carbon Fibers*; Peng, J.C.M.; Donnet, J.B.; Wang, T.K.; Rebouillat, S., Ed.; Marcel Dekker: New York, **1998**, 3, 161.
18. Herrera-Franco, P.J.; Drzal, L.T., Comparison of methods for the measurement of fibre/matrix adhesion in composites. *Composites*, **1992**, 23(1), 2-27.

19. Pearson, H.A.; Andrie, J.M; Urban, M.W., Covalent attachment of multilayers (CAM): a platform for pH switchable antimicrobial and anticoagulant polymer surface. *Biomaterials Science*, **2014**, 2(4), 512-521.
20. Pittman, C.U.; He, G.R.; Wu, B.; Gardner, S.D., Chemical modification of carbon fiber surfaces by nitric acid oxidation followed by reaction with tetraethylenepentamine. *Carbon*, **1997**, 35(3), 317-331.
21. Xu, B.; Wang, X.; Lu, Y., Surface modification of Polyacrylonitrile-based carbon fiber and its interaction with imide. *Applied Surface Science*, **2006**, 253(6), 2695-2701.
22. Marcandalli, B.; Riccardi, C. Plasma treatments of fibres and textiles. *Plasma technologies for textiles*; Shishoo, R., Ed.; Woodhead: Cambridge, 2007, 282.
23. Yue, Z.R.; Jiang, W.; Wang, L.; Gardner, S.D.; Pittman, C.U., Surface characterization of electrochemically oxidized carbon fibers. *Carbon*, **1999**, 37(11), 1785-1796.
24. Delamar, M.; Desarmot, G.; Fagebaume, O.; Hitmi, R.; Pinsonc, J.; Savéant, J.M., Modification of carbon fiber surfaces by electrochemical reduction of aryl diazonium salts: Application to carbon epoxy composites. *Carbon*, **1997**, 35(6), 801-807.
25. Downard, A.J., Electrochemically assisted covalent modification of carbon electrodes. *Electroanalysis*, **2000**, 12(14), 1085-1096.
26. Wu, G.M., Oxygen plasma treatment of high performance fibers for composites. *Materials Chemistry and Physics*, **2004**, 85(1), 81-87.

27. Chen, C.; Liang, B.; Ogino, A.; Wang, X.; Nagatsu, M., Oxygen functionalization of multiwall carbon nanotubes by microwave-excited surface-wave plasma treatment. *The Journal of Physical Chemistry C*, **2009**, *113*(18), 7659-7665.
28. Graham, W.G. The physics and chemistry of plasmas for processing textiles and other materials. *Plasma technologies for textiles*; Shishoo, R., Ed.; Woodhead: Cambridge, 2007, 1.
29. Yasuda, H.; Hsu, T., Some aspects of plasma polymerization investigated by pulsed RF discharge. *Journal of Polymer Science: Polymer Chemistry Edition*, **1977**, *15*(1), 81-97.
30. Thompson, L.F.; Mayhan, K.G., The plasma polymerization of vinyl monomers. II. A detailed study of the plasma polymerization of styrene. *Journal of Applied Polymer Science*, **1972**, *16*(9), 2317-2341.
31. Kobayashi, H.; Bell, A.T.; Shen, M., Plasma polymerization of saturated and unsaturated hydrocarbons. *Macromolecules*, **1974**, *7*(3), 277-283.
32. Ryan, M.E.; Hynes, A.M.; Badyal, J.P.S., Pulsed plasma polymerization of maleic anhydride. *Chemistry of Materials*, **1996**, *8*(1), 37-42.
33. Xie, Y.; Sherwood, P.M., X-ray photoelectron-spectroscopic studies of carbon fiber surfaces. Part IX: the effect of microwave plasma treatment on carbon fiber surfaces. *Applied Spectroscopy*, **1989**, *43*(7), 1153-1158.
34. Aumsuwan, N.; Heinhorst, S.; Urban, M.W., Antibacterial Surfaces on Expanded Polytetrafluoroethylene (ePTFE); Penicillin Attachment. *Biomacromolecules*, **2007**, *8*(2), 713-718.

35. R.A. Wolf, R.A. *Atmospheric pressure plasma for surface modification*. John Wiley & Sons: Hoboken, **2013**.

CHAPTER TWO

RESEARCH OBJECTIVE

The objective of this thesis is to understand the role of fiber-matrix interface and utilizing microwave plasma surface modifications (MPSM) design interfaces that will result in enhanced composite mechanical properties and to develop technologically feasible, inexpensive, and clean surface modifications. This interface is critical because the mechanical properties are determined by how the interface is able to distribute the load properly throughout the composite. If the load is not distributed properly by the interface, the composite will have premature failure. As discussed in Section 1.4, carbon fibers suffer from inherent surface inertness, which makes it difficult for the matrix to adhere onto the carbon fiber surface.

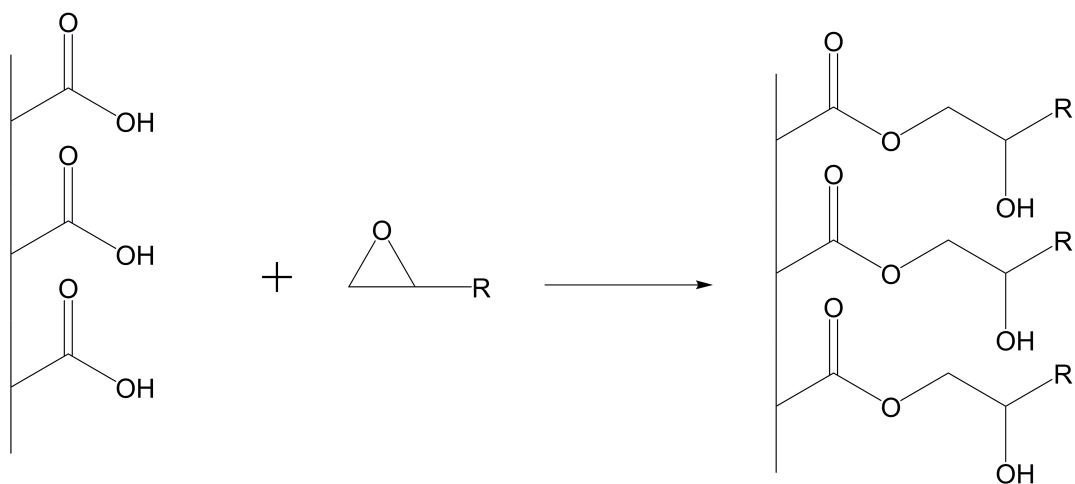


Figure 2.1: Hydroxyl groups from a modified carbon fiber surface reacting with an epoxy group to form chemical bonds.

A solution to this obstacle is to utilize surface modifications to introduce chemical functional groups onto the surface to enhance and promote fiber-matrix interactions, which is illustrated in Figure 2.1; furthermore, MPSM was chosen to explore the effects on carbon fiber surfaces compared to other surface modification techniques. MPSM will be utilized because the system does not affect the bulk properties, solvent free, and promotes high chemical reactivity. The functional groups that will be generated from this process will be carboxylic acid (-COOH) and alcohol (-OH) groups, so they can facilitate further reactions involving an epoxy matrix. The unmodified carbon fiber surfaces (PAN-based) will be modified by microwave plasma utilizing two different approaches to observe the generation of these chemical functional groups. The first approach will be to subject the PAN-based fibers to only argon gas (MPAr) reactions, which will act as the control experiment. The second approach will be to subject the PAN-based fibers in the presence of maleic anhydride monomer and argon gas (MPMA) reactions. These conditions will be critical since both conditions will generate functional groups that can be enhance the fiber-matrix interface. The MPMA and MPAr reacted fiber surfaces will be examined by monitoring the changes through surface characterization and mechanical testing. The surface characterization techniques used were Raman and Attenuated Total Reflectance-Fourier Transform Infrared spectroscopy (ATR-FTIR). Raman spectroscopy will monitor how MPMA and MPAr affect the D-band and G-band present on the carbon fiber surfaces, which is discussed in Section 1.2. ATR-FTIR spectroscopy will analyze the formation of -COOH and -OH groups on the MPMA and MPAr reacted surfaces. The mechanical properties will be measured through a microbond technique to see the extent

of how the modified surfaces affected the fiber-matrix interface. The microbond technique will measure the interfacial shear stress between the fiber and the matrix, which will be further discussed in the forthcoming chapters. The hypothesis for this research is that the microwave plasma enhanced interface surfaces (MPMA and MPAr) will show an improvement to interfacial shear stress compared to PAN-based fibers, and will lead to a better composite.

CHAPTER THREE

RESEARCH METHODOLOGY

3.1 MATERIALS

The carbon fibers, 3 k tow with epoxy sizing, were purchased from ACP Composites and cut to 5 cm lengths. The maleic anhydride monomer was purchased from TCI America and stored in a desiccator until utilized. The epoxy matrix utilized was 1100 UV clear coat resin – Part A and 1100 UV clear coat hardener – Part B purchased from Fiberlay. Ultra-high purity argon gas was purchased from Airgas.

The pre-cut carbon fibers were washed before the experiment to remove any contaminants.^{1,2} Pre-cut carbon fibers were placed into 20 mL vials and washed in three solvents: acetone, de-ionized water, and isopropanol. Each solvent wash was a fifteen-minute process in an ultrasonic bath. After the initial wash, this process was repeated twice; a total of two hours and fifteen minute procedure. The carbon fibers were then placed into a 45°C oven and stored in a desiccator until utilized.

3.2 MICROWAVE PLASMA SYSTEM DESIGN

Microwave plasma reactions were conducted as an open reaction system based on a method previously reported.³ The vacuum was continuously pulled during the reaction to prevent pressure build up. Figure 3.1 illustrates a schematic diagram of the microwave plasma system.

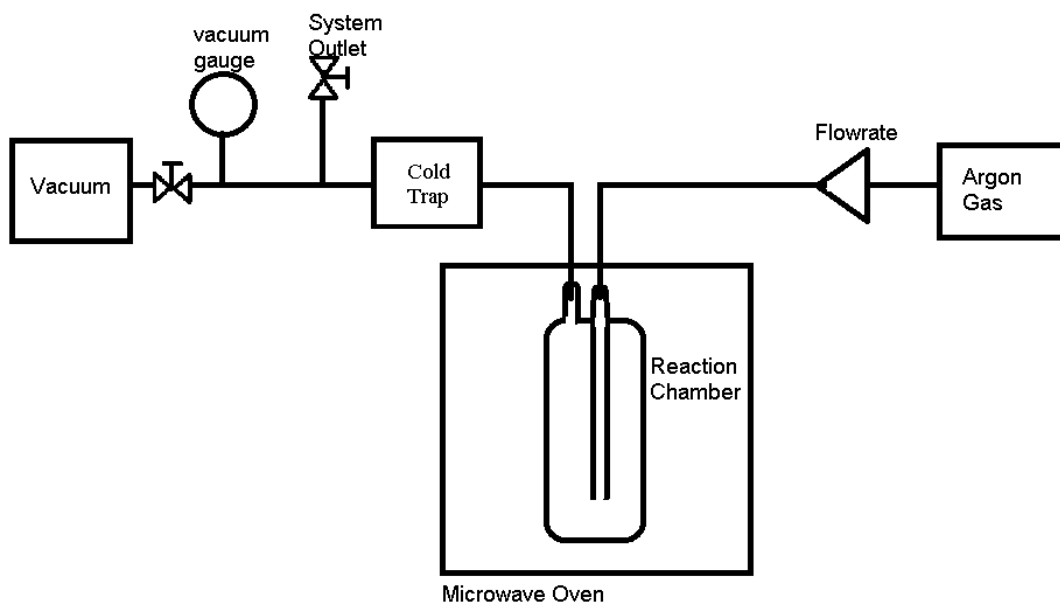


Figure 3.1: Schematic diagram of the microwave oven plasma system.

On the left side of the figure, the system is continuously under vacuum and a vacuum gauge was utilized to monitor the system's pressure in inHg. Between the vacuum and cold trap were two valves. The first valve controlled the vacuum and the second valve released the vacuum, allowing the reaction chamber to return to atmospheric pressure. The cold trap was utilized to condense the vapors that were pulled from the reaction chamber during the reaction, which was the maleic anhydride vapor and argon gas. The reaction chamber inside the microwave was set up so that the inner tube had the argon gas flowing straight into the end of the chamber, where the maleic anhydride (MA) monomer would be placed, while the second tube was connected to the vacuum line. The purpose of this setup was to allow the plasma to react with the MA monomer before interacting with the substrate. On the right side of the figure, the argon gas entered the system controlled by a flowmeter.

3.3 MICROWAVE SURFACE MODIFICATION PROCEDURE OF CARBON FIBERS

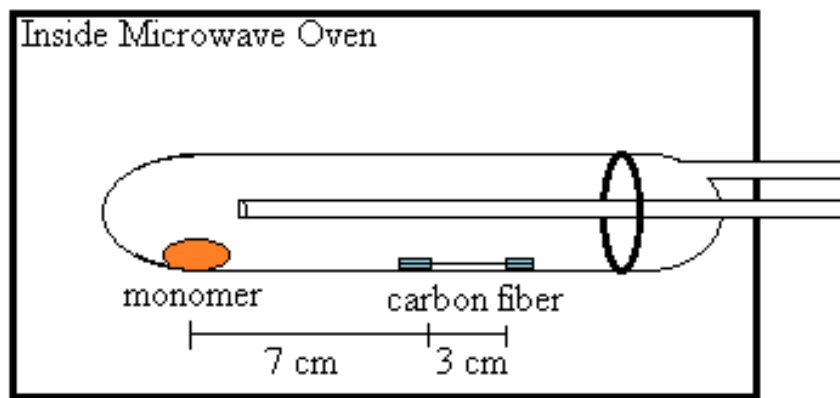


Figure 3.2: Schematic diagram of reaction chamber during MPMA reaction.

The plasma operations for an open reaction chamber were described elsewhere.^{3,4} In this experiment, shown in Figure 3.2, the MA monomer (200 mg) was loaded into the reaction chamber at the far end. The fibers were loaded into the chamber 7 cm away from the end on glass platforms and 3 cm of the fiber surfaces were exposed for surface modification. The glass platforms allowed the fibers to be hung horizontally and hanging the fibers would ensure that the plasma would modify all of the exposed surface area of the fibers. The chamber was evacuated under vacuum to 50-250 mTorr to purge the reaction chamber, which was followed by two flushes of argon gas before introducing a low flowrate of argon gas that would reach equilibrium within the chamber. In order for the plasma to be generated, the microwave had to have an output of 1,250 W and produce an output frequency of 2.45 GHz. The microwave timer was set to 7 seconds, but the actual plasma produced was only generated for an average of 3.59 \pm 0.18 seconds. During the reactions, two observations were made about the MPMA and MPAr reactions.

The MPAr would produce a pinkish discharge glow, while MPMA would produce a blue-white discharge glow.

3.4 ANALYTICAL METHODS

3.4.1 Attenuated Total Reflectance-Fourier Transform Infrared Spectroscopy (ATR-FTIR)

For surface characterization of the carbon fibers, ATR-FTIR spectroscopy was utilized. The spectra were collected using Agilent Cary 680 FTIR equipped with 2 mm diamond ATR crystal. The spectrum resolution was set at 4 cm^{-1} , and the background and sample spectrum were collected by co-adding 64 scans for each. The ATR-FTIR will be utilized as an important instrument to monitor functional group formation on the carbon fiber surfaces.⁵

3.4.2 Raman Spectroscopy

The Raman spectra were collected on Reinshaw in-Via Raman microscope that was equipped with a 785 nm diode laser. The microscope was equipped with a computer controlled three-axis encoded (X, Y, Z) motorized stage, a RenCam CCD detector, and a Leica microscope (DM2500M). The maximum excitation source was 300 mW. The collection of the spectra was set at an acquisition time of 10 seconds with 10 accumulations using 30 mW laser power. The spectrum resolution was 1 cm^{-1} . For each specimen, three Raman spectra were collected along the length of the fibers to ensure chemical homogeneity of surface modification. Raman spectra produced were utilized to study the D-band and G-band of the carbon fibers.⁶

3.4.3 Microbond Technique

A microbond technique was utilized to evaluate the effects of surface modifications by measuring the interfacial shear stress (τ_i). This experiment was conducted by embedding a single fiber into an epoxy matrix, as shown in Figure 3.3. A force (F_D) was applied to pull the fiber from one end until the fiber debonds from the encapsulated epoxy bead. By measuring the shear stress, which was calculated by dividing F_D by the imbedded surface area⁷ (Eqn. 3.1), this measured the interfacial shear stress between the fiber and the matrix. It was important to compare the shear stress for PAN-based, MPMA, and MPAr reactions, because it demonstrated the extent of how much the surface modifications affected the interfacial shear stress.⁷

$$\tau_i = \frac{F_D}{\pi d l_B} \quad (3.1)$$

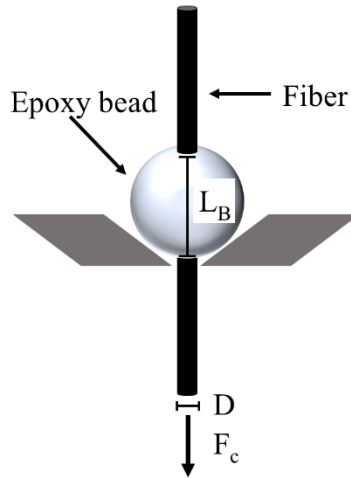


Figure 3.3: Schematic diagram of the microbond set up for single fiber pull out. The shear stress measurements were prepared by separating the 3 k carbon fiber bundle into single fibers. Single fibers were for PAN-based, MPMA, and MPAr reacted bundles. A single fiber was stretched onto a paper tab and held in place by glue. The epoxy bead

was made by mixing equal parts in volume (1:1) of the 1100 UV clear coat resin – Part A and 1100 UV clear coat hardener – Part B per the instructions from the manufacturing company. The epoxy solution was then degassed under vacuum for an hour to eliminate bubbles that were formed. After degassing, the epoxy was applied to the single carbon fiber using a wire to create the epoxy microbead, which is illustrated in Figure 3.4.

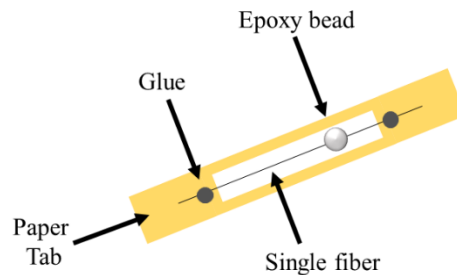


Figure 3.4: Epoxy bead on a single fiber prepared for testing.

The sample was analyzed under a microscope to observe and capture images of the embedded length and the diameter of the fiber. Digital image software was utilized to obtain the length and diameter for shear stress calculation. The paper tab was punctured with a hole that is furthest away from the epoxy bead to hang the hangar that was used to apply the force. The epoxy bead was carefully placed between the caliper opening of 100 microns so that the epoxy microbead was holding the single fiber, paper tab, and hangar illustrated in Figure 3.5.⁵

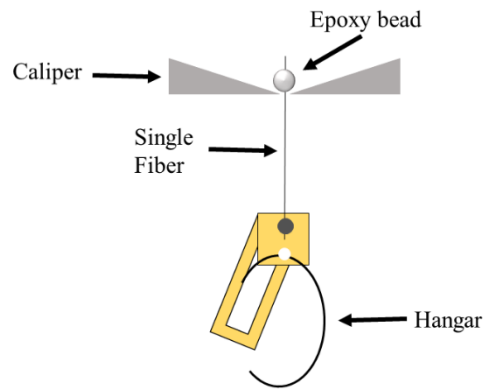


Figure 3.5: Schematic diagram of microbond single fiber experiment.

The weight was added to the hangar until the de-bonding force was achieved causing the single fiber to de-bond from the epoxy microbead, allowing a calculation of interfacial shear stress.

REFERENCES

1. Xu, B.; Wang, X.; Lu, Y., Surface modification of polyarylonitrile-based carbon fiber and its interaction with imide. *Applied surface science*, **2006**, 253(6), 2695-2701.
2. Severini, F.; Formaro, L.; Posca, L., Chemical modification of carbon fiber surfaces. *Carbon*, **2002**, 40(5), 735-741.
3. Gaboury, S.R.; Urban, M.W., Quantitative attenuated total reflectance Fourier transform infrared analysis of microwave plasma reacted silicone elastomer surfaces. *Langmuir*, **1994**, 10(7), 2289-2293.
4. Kim, H.; M.W. Urban, M.W., Microwave Plasma Reactions of Imidazole on Poly(dimethylsiloxane) Elastomer Surface: A Spectroscopic Study. *Langmuir*, **1995**, 11(6), 2071-2076.
5. Urban, M.W. *Vibrational Spectroscopy of Molecules and Macromolecules on Surfaces*. John Wiley & Sons: New York, **1993**.
6. Koenig, J.L. *Spectroscopy of Polymers*. Elsevier: New York, **1999**.
7. Herrera-Franco, P.J.; Drzal, L.T., Comparison of methods for the measurement of fibre/matrix adhesion in composites. *Composites*, **1992**, 23(1), 2-27.

CHAPTER FOUR

RESULTS AND DISCUSSION

This chapter is divided into sections: Chemical Analysis of Surface Modified Carbon Fibers (4.1), Mechanical Analysis of Fiber-Matrix Interfaces (4.2), Correlation of Spectroscopic and Mechanical Analysis (4.3), Summary and Correlation to Composite Mechanical Properties (4.4), and Summary and Future Work (4.5) . Chemical Analysis of Surface Modified Carbon Fibers describes how surface characterization techniques are utilized to analyze the modified surfaces. This section analyzes Raman and ATR-FTIR spectroscopy data obtained from microwave plasma surface modifications of carbon fiber surfaces in the MPMA and MPAr reactions. These results will be used to propose the mechanism for the MPMA and MPAr reacted carbon fiber surfaces. The Mechanical Analysis of Fiber-Matrix Interfaces will address the role of interfacial modifications on mechanical properties of composites. The method utilized to demonstrate the enhanced interface through interfacial shear stress measurements. Correlation of Spectroscopic and Mechanical Analysis will address the relationship between molecular level interfacial chemistry generated by MPMA and MPAr modified fibers and mechanical shear stress measurements. Finally, the correlation between mechanical properties of carbon fiber composites and surface modifications will be made.

4.1 CHEMICAL ANALYSIS OF SURFACE MODIFIED CARBON FIBERS

The objective of this research is to enhance the interface between the fiber-matrix by subjecting PAN-based carbon fiber surfaces to MA monomer and Ar gas using a microwave plasma process to alter the surface chemistry.¹ Microwave surface modifications were analyzed by using surface characterization techniques to monitor the alterations of the carbon fiber surfaces. This was accomplished by utilizing Raman and ATR-FTIR spectroscopy.

4.1.1 Raman spectroscopy analysis of MPMA and MPAr reactions

Section 1.2 discussed hybridization and crystal lattice structure on the surface of carbon material. This was important because MPSM can affect the hybridization and the crystal lattice. The MPSM process changes the hybridization from sp^2 to sp^3 , which would also indicate that the crystal lattice is converted from graphitic to amorphous structures. This change is demonstrated in Figure 4.1.

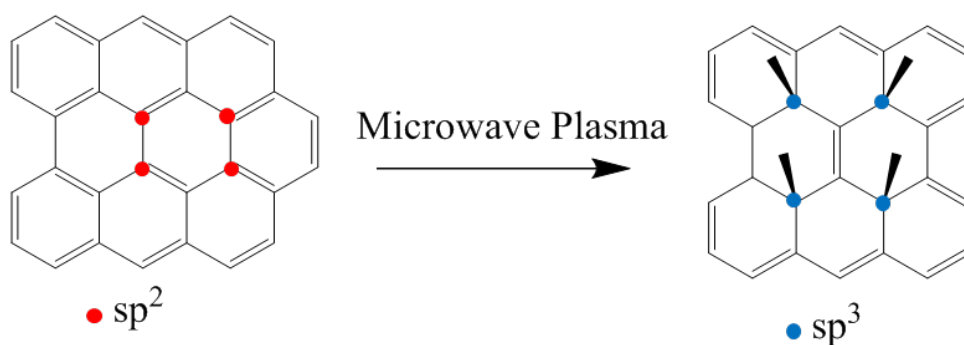


Figure 4.1: Schematic diagram of sp^2 to sp^3 carbon fiber surfaces hybridization.

As microwave plasma reacts with the aromatic rings, the sp^2 hybridization is converted to sp^3 hybridization because the generated plasma will interact with the double bonds during the reaction. These changes can be monitored using Raman spectroscopy because there

are two distinct bands that exist within the carbon fiber spectra. These bands are named as D-band, detected in the 1330-1350 cm^{-1} region, and G-band, detected in the 1580 cm^{-1} region. The D-band is due to the presence of disordered structures. While the G-band is related to the graphitic structures present, which has a hexagonal close-packed crystal lattice structure. The area under the D-band (I_D) is attributed to sp^3 hybridization, and the area under the G-band (I_G) is attributed to sp^2 hybridization. If there was an increase of I_D then it would indicate an increase of sp^3 hybridization. This would also mean a decrease in sp^2 hybridization and I_G . This indicates an overall change of amorphous structures present on the surface. If there was a decrease of I_D and an increase in I_G , then this would indicate that the surface would be more graphitic. Thus a ratio can be established between I_D/I_G which is utilized to determine if the microwave plasma process altered the surface to be more amorphous or graphitic. Raman spectroscopic data was collected for PAN-based, MPMA reacted, and MPAr reacted carbon fiber surfaces, an example of these spectra are shown in Figure 4.2, (a) (b) and (c). Each Raman spectra was baseline corrected and deconvoluted into four different bands: G-band (1580 cm^{-1})³, D-band (1350 cm^{-1})³, D3-band (1500 cm^{-1})³ and D4-band (1200 cm^{-1})³. The D3-band and D4-band are due to amorphous carbon and disordered graphitic carbon that are present in carbon materials³ and was added to obtain a better curve fit. Table 4.1 shows a summary of the results of the I_D/I_G ratio changes for PAN-based, MPMA, and MPAr from multiple spectra.

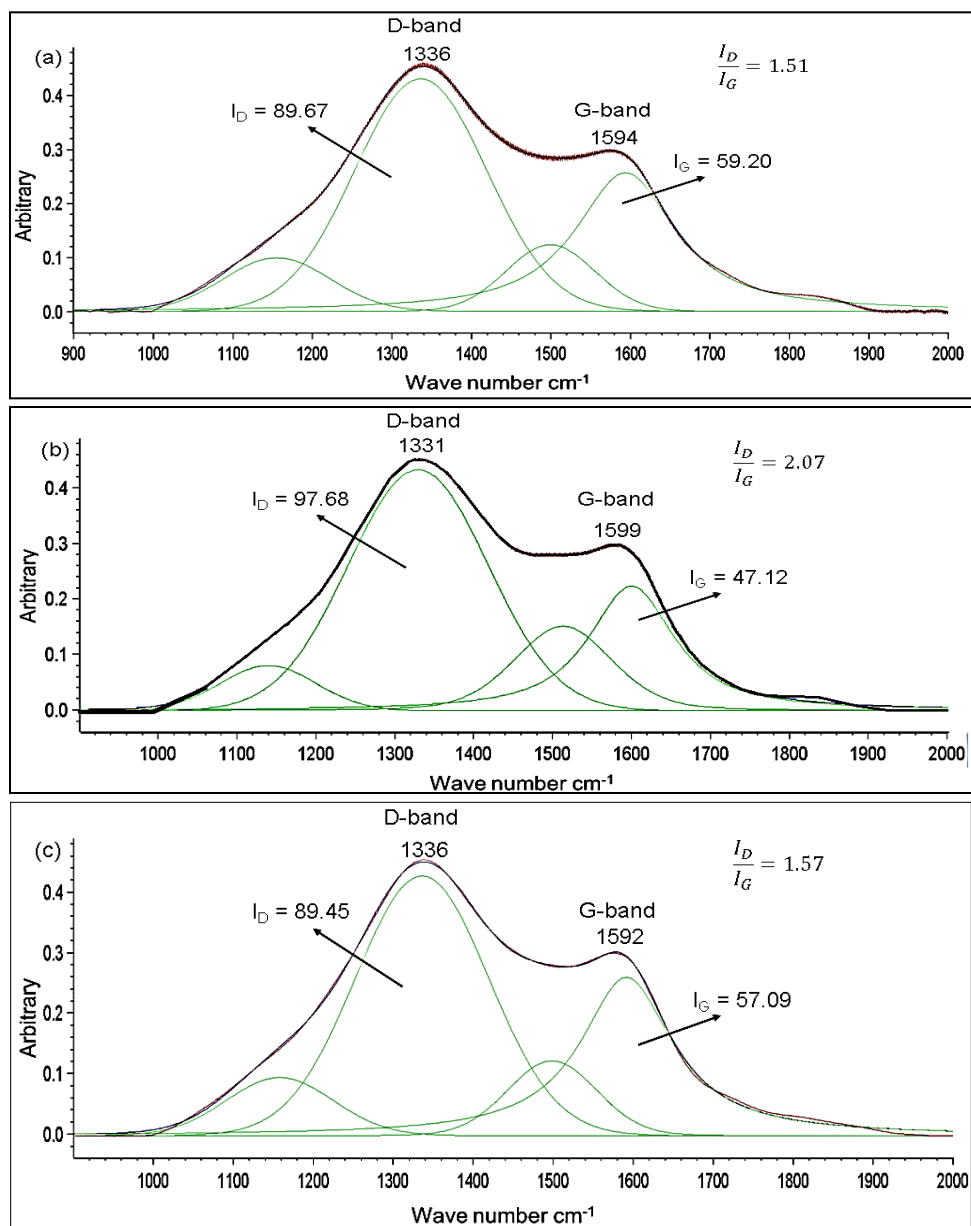


Figure 4.2: Raman spectrum curve fitting was utilized to determine I_D to I_G ratios of (a) PAN-based, (b) MPMA, and (c) MPAr fibers.

Table 4.1: Average Area of D over G bands for PAN-based, MPMA, and MPAr.

	D – band (cm ⁻¹)	G – band (cm ⁻¹)	I _D /I _G Ratio
PAN-based	1328	1594	1.36 ±0.23
MPMA	1330	1595	1.99 ±0.19
MPAr	1330	1593	1.30 ±0.19

The PAN-based carbon fibers had an average I_D/I_G of 1.36 ±0.23 while the MPMA and MPAr reacted had an average I_D/I_G of 1.99 ±0.19 and 1.30 ±0.19. The MPMA reaction had an overall increase in the I_D/I_G ratio, which was attributed to the conversion of sp² to sp³ hybridization and the introduction of defects. The MPAr reaction resulted in an overall slight decrease compared to PAN-based, which indicates that the surface as more graphitic. These results show the effects of microwave plasma reactions on the surface structures were semi-quantified by utilizing Raman spectroscopy; however, Raman spectroscopy is unable to determine the functional groups that were generated on the fiber surface. ATR-FTIR was utilized to determine the functional groups.

4.1.2 ATR-FTIR spectroscopy analysis of MPMA and MPAr reactions

The surface of the carbon fiber was further analyzed using ATR-FTIR to monitor the generation of functional groups on the altered carbon fiber surfaces. In previous works^{4,5}, maleic anhydride was analyzed through ATR-FTIR by monitoring the formation of carbonyl groups (C=O), -OH and -COOH to indicate surface functionalization. In the ATR-FTIR spectra, the following bands were analyzed: 3600, 2597, 1740, 1600, 1450, 1350, 1250, and 1150 cm⁻¹. The regions 1740, 1350, 1250, and 1150 cm⁻¹ are vibrational bands that are associated with the C=O, C-O, and -OH bonds. The 1600 cm⁻¹ band vibration is associated with the conjugated double bond (C=C) that

is found in the aromatic rings. These regions provided the functionality being generated on the carbon fiber surface by MPSM. The carbon fiber surface was analyzed before and after MPSM, the spectra were baseline corrected and normalized at 900 cm^{-1} to monitor intensity changes.

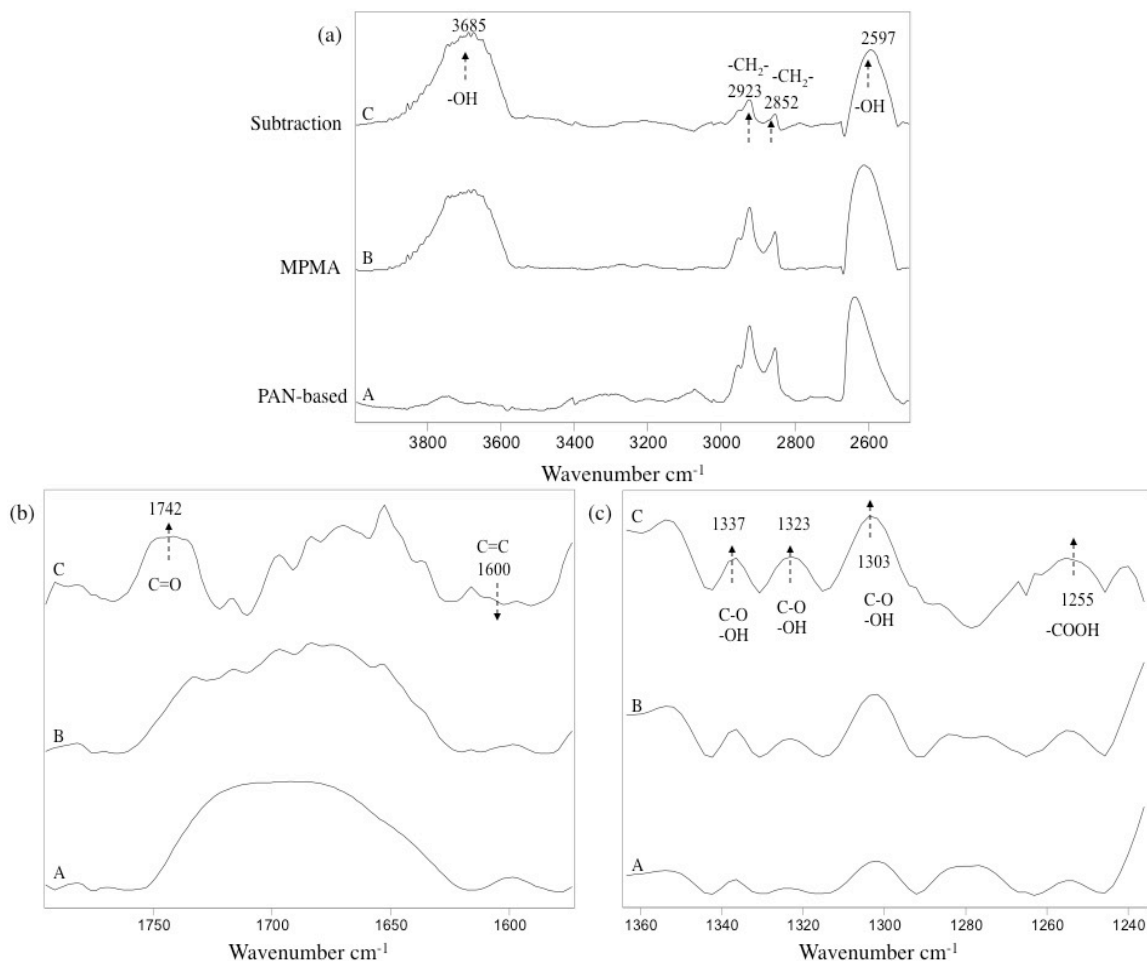


Figure 4.3: ATR-FTIR spectra of MPMA carbon fibers in the (a) $3800\text{-}2600\text{ cm}^{-1}$ (b) $1750\text{-}1600\text{ cm}^{-1}$ and (c) $1360\text{-}1200\text{ cm}^{-1}$ regions.

Trace A is the spectra of PAN-based fibers. Trace B is the spectra of the MPMA reactions. Trace C is the subtraction spectra. As shown, the band at 1748 cm^{-1} increases which is attributed to C=O stretching vibrations of carboxylic acid of the MA. The bands

at 1600 cm^{-1} indicates a decrease in conjugated C=C aromatic stretching vibrations due to the bond cleavage initiated by plasma. In Figure 4.3 (b), the bands at 1337, 1323, 1303 cm^{-1} exhibit an increase, which is attributed to either C-O band vibrations or -OH deformation vibrations in carboxylic acid and ester functional groups.^{6,7,8} This is also manifested by the increase of -COOH band at 1253 cm^{-1} .^{6,7,8} Additionally, the bands at 3685 and 2597 cm^{-1} exhibit an increase attributed to -OH vibrations that occurs to -COOH.^{6,7,8} These results confirm that carboxylic acid groups were formed onto the surface of the carbon fibers through the MPMA reaction.

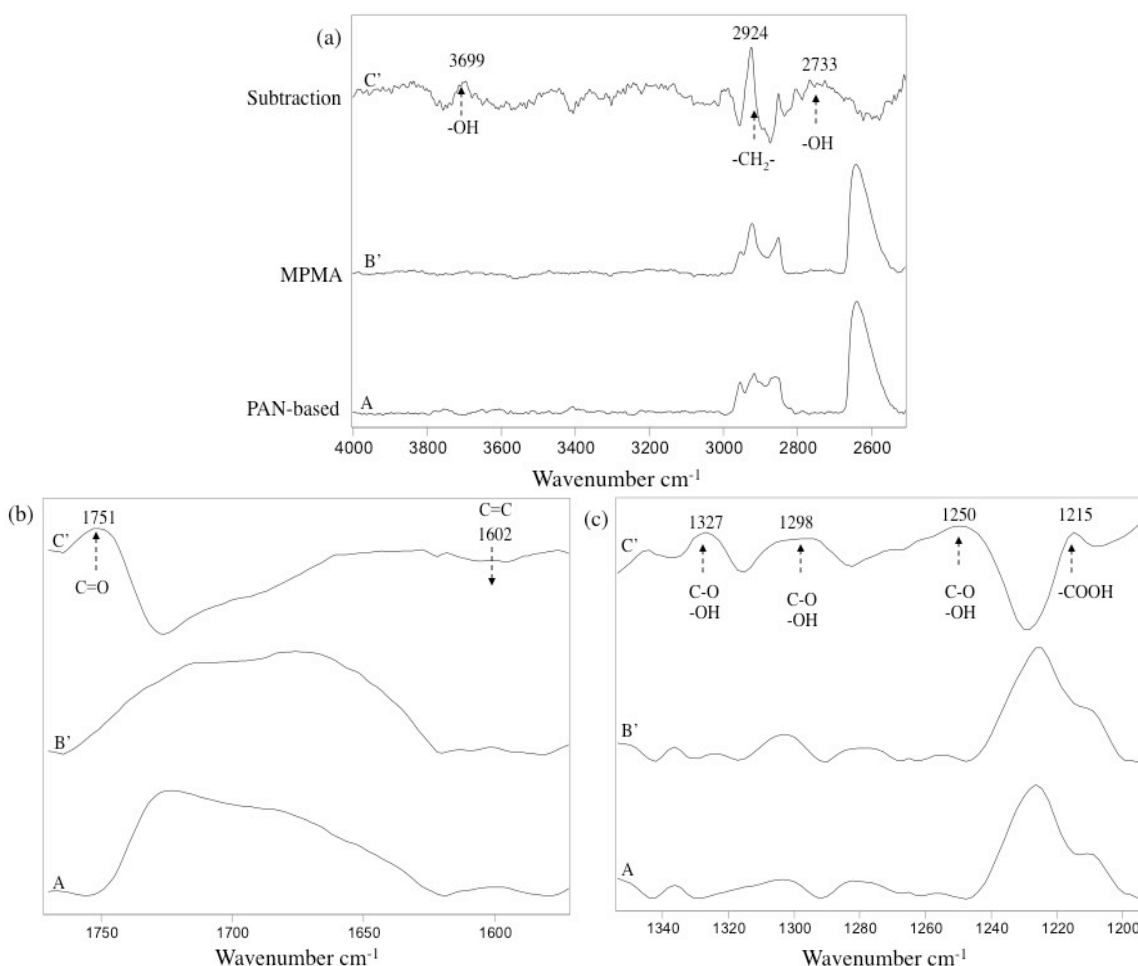


Figure 4.4: ATR-FTIR spectra of MPAr fibers in the (a) 4000-2600 cm^{-1} (b) 1750-1600 cm^{-1} and (c) 1350-1200 cm^{-1} regions.

Trace A is the spectra of PAN-based fibers. Trace B' is the spectra of the MPAr reactions. Trace C' is the subtraction spectra. As shown, the 1751 cm^{-1} band, in Figure 4.4a, indicates an increase in the C=O stretching vibration that is attributed to MA. The band at 1602 cm^{-1} indicates a slight decrease to the C=C aromatic stretching vibrations, which is attributed to bonds being cleaved during the MPAr reaction. In Figure 4.4 (b), the bands at 1327, 1298, 1250 cm^{-1} exhibit a slight increase, which is attributed to C-O and -OH deformation vibrations.^{6,7,8} The -OH band vibration can be observed as a slight

increase at 3699 and 2733 cm^{-1} . This is also manifested by a slight increase of -COOH band at 1215 cm^{-1} .^{6,7,8} These results show that carboxylic acid and alcohol functional groups were generated on the carbon fiber surfaces. The MPAr and MPMA surface modifications resulted in similar bands that appeared in Trace C and Trace C'. In Trace C, the band at 1748 cm^{-1} indicates an increase attributed to C=O carboxylic acid vibrations and is supported by the band 1253 cm^{-1} which is attributed to -COOH carboxylic acid vibrations. Other bands that support the formation of carboxylic acid on the surface are the bands 1337, 1323, and 1304 cm^{-1} , which indicates an increase attributed to -OH vibrations. There is a band at 1613 cm^{-1} that is attributed to C=C aromatic stretching vibrations that decreases after the surface modification. In Trace C', the band at 1751 cm^{-1} indicates an increase attributed to C=O carboxylic acid vibrations and is supported by the bands at 1253 and 1209 cm^{-1} , which is attributed to -COOH carboxylic acid vibrations. Other bands that support the formation of carboxylic acid on the surface are the bands at 1326 and 1296 cm^{-1} , both of which indicate an increase attributed to -OH vibrations. There is a band at 1599 cm^{-1} that is attributed to C=C aromatic stretching vibrations that decreases after the surface modification. Even though the MPMA and MPAr have similar band vibrations after the surface modification, the MPMA exhibited an increase in -CH₂- bending vibrations at 1458 cm^{-1} that was not present in the MPAr, illustrated in Figure 4.5.

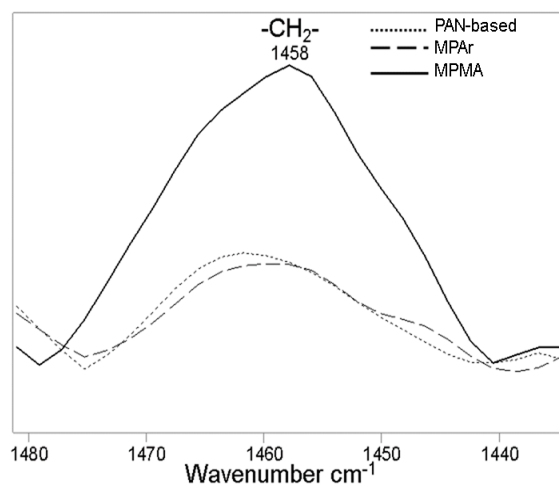


Figure 4.5: CH_2 bending region of PAN-based, MPAr, and MPMA fibers.

The presence of $-\text{CH}_2-$ alludes to how the MA monomer is attached to the surface of the carbon fibers. During the MPMA reaction, the $\text{C}=\text{C}$ bond was cleaved in the MA monomer which resulted in free radicals being formed to react to the carbon fiber surface. The $\text{C}=\text{C}$ bond was cleaved because Trace B, in Figure 4.3a, indicated a decrease in the $\text{C}=\text{C}$ band vibrations at the band 1613 cm^{-1} compared to Trace A. Furthermore, the created radicals on the surface reacted with a radical from the MA monomer to form a covalent bond. The second radical, on the MA monomer, underwent hydrogen protonation to form the $-\text{CH}_2-$ band at 1458 cm^{-1} . As a result, Figure 4.6 ideally illustrates how the MA monomer attached to the carbon fiber surfaces after the reaction. The monomer attachment is supported by the Raman spectroscopy, in Figure 4.2b, because the attachment creates defects on the surface, which resulted in an increase of the I_D/I_G ratio.

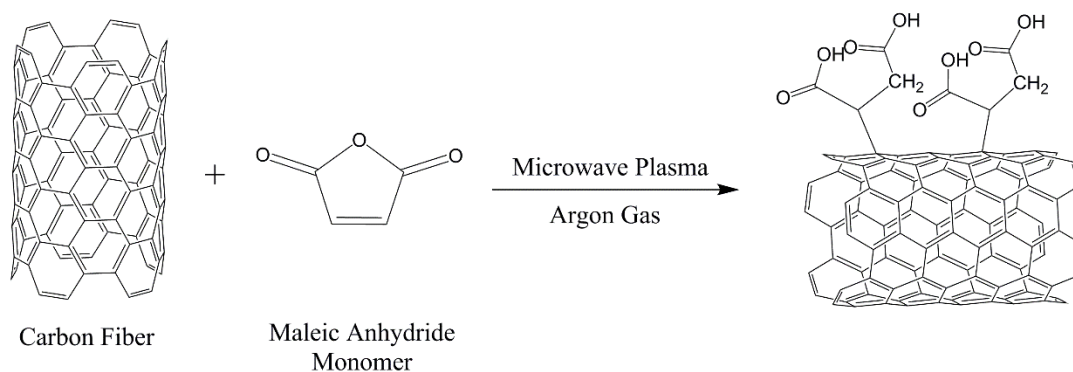


Figure 4.6: MPMA reactions to carbon fiber surfaces.

MPAr has a similar mechanism to MPMA, but it is different due to how the functional groups are generated on the altered surface. During the reaction, the plasma etched by the charged particles interacts with the surface of the carbon fibers to cleave the C=C bonds and form free radicals. Since argon is an inert gas, the free radicals produced from the plasma cannot react with anything present in the chamber until it becomes exposed from air.⁹ The functional groups generated from air exposure are similar to MA because the free radicals react with the oxygen in air.¹⁰ However, the Raman spectra, as shown in Figure 4.2c, resulted in no hybridization changes after the carbon fibers were exposed to MPAr reactions. The lack of hybridization changes suggests that the plasma etched the surface therefore removing a layer of the carbon to expose a more graphitic layer that was reacted. The graphitic layer was exposed to the charged particles that created free radicals that reacted with air. In a different plasma study it is suggested that since argon gas is inert, the plasma would change the physical aspects of the surface and not overly affect the surface chemistry.^{11,12} ATR-FTIR surface characterization illustrated how MPMA and MPAr altered the carbon fiber surfaces. The spectra showed the difference in the MPMA and MPAr reaction and how they could be differentiated. Utilizing ATR-FTIR

and Raman spectroscopic data, a plausible mechanism can be established on how microwave plasma reactions and changes the overall surface chemistry of the carbon fibers that will lead to an enhanced interface.

4.1.3 Proposed mechanism for MPMA and MPAr surface modifications

Microwave plasma surface modifications chemically altered the PAN-based carbon fiber surfaces, which was characterized by ATR-FTIR and Raman spectroscopy. Section 4.1.2, Raman spectroscopy semi-quantified the surface modifications by monitoring the I_D/I_G ratio. The ratio measured the hybridization conversion from sp^2 to sp^3 after the surface modification. As a result, an increase in I_D/I_G ratio indicated an increase in defect sites being generated and a decrease in I_D/I_G ratio indicated graphitic surfaces were exposed. Section 4.1.3 discussed how ATR-FTIR spectroscopy monitored the generation of functional groups which were -COOH, C=O, and -OH. Also, the spectra gave an indication of how the MPMA and MPAr reactions generated the similar functional groups on the surface, but the reactions could be differentiated. Raman and ATR-FTIR spectroscopic data were used to propose a mechanism of how microwave plasma induced the chemical alterations to the carbon fiber surfaces. Microwave plasma generates charged particles that collide into the surface to form free radicals; however, the MPMA and MPAr diverge into different mechanisms that will be discussed. In the MPMA reaction, illustrated in Figure 4.7a, the free radicals cleave the conjugated C=C bonds on the carbon fiber surfaces and the C=C bond in the maleic anhydride monomer. The decrease of these conjugated C=C bonds are shown as band vibrations and vibrations in ATR-FTIR spectroscopy. A radical from the MA monomer reacts with another radical

from the surface of the carbon fibers to form a covalent bond. The newly formed bond is seen in Raman spectroscopy as a change in the surface hybridization from sp^2 to sp^3 . Raman spectroscopic data indicated that the I_D/I_G ratio increased, which means that the amount of amorphous sp^3 hybridization increased. The anhydride ring opens by hydrolysis to produce the $-COOH$ groups when it was exposed to the moisture in the air. The second free radical, on the MA, experiences hydrogen protonation to produce a $-CH_2-$. This protonation is supported by the appearance of the $-CH_2-$ band vibration at 1458 cm^{-1} . In the MPA_r reaction, illustrated in Figure 4.7b, the free radicals cleave the conjugated $C=C$ bonds on the carbon fiber surfaces. This is seen as a decrease in the $C=C$ band vibrations in ATR-FTIR spectroscopy. The functional groups that were generated through this reaction formed after the free radicals were exposed to air.

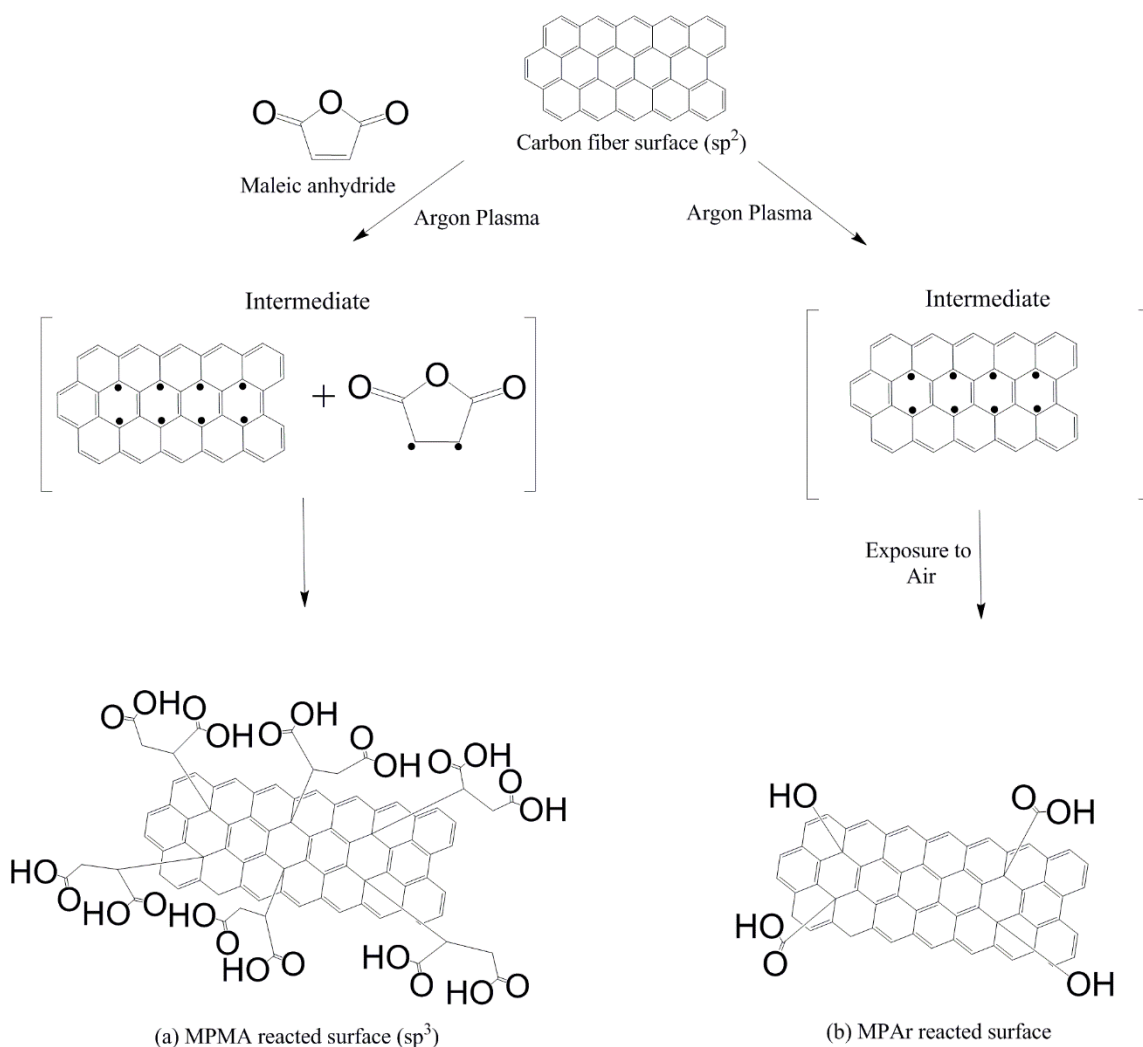


Figure 4.7: Proposed mechanism for MPMA and MPAr reactions to carbon fiber surfaces.

MPMA and MPAr reactions established a mechanism behind the microwave plasma process by utilizing ATR-FTIR and Raman spectroscopic data. The ATR-FTIR spectroscopy results showed what functional groups were generated onto the carbon fiber surfaces. Raman spectroscopy focused on the surface structure by utilizing the I_D/I_G ratio relationship, which was related to the changes in hybridization. As the sp^2 converted to

sp³ this indicated that the graphitic crystal structure was being converted to amorphous diamond crystal structures.

4.2 MECHANICAL ANALYSIS OF FIBER-MATRIX INTERFACES

The objective of this part of the research is to use microwave plasma surface modifications to enhance the fiber-matrix interface by generating -COOH and -OH functional groups. This interfacial interaction enhances how the matrix interacts with the former inert carbon fiber surface. The functional groups reacted with the matrix to form chemical bonds which will decrease de-bonding from occurring within the composite. Figure 4.8 illustrates how the MPMA and MPAr reactions would enhance the interface by reacting the epoxy ring with the hydroxyl groups.

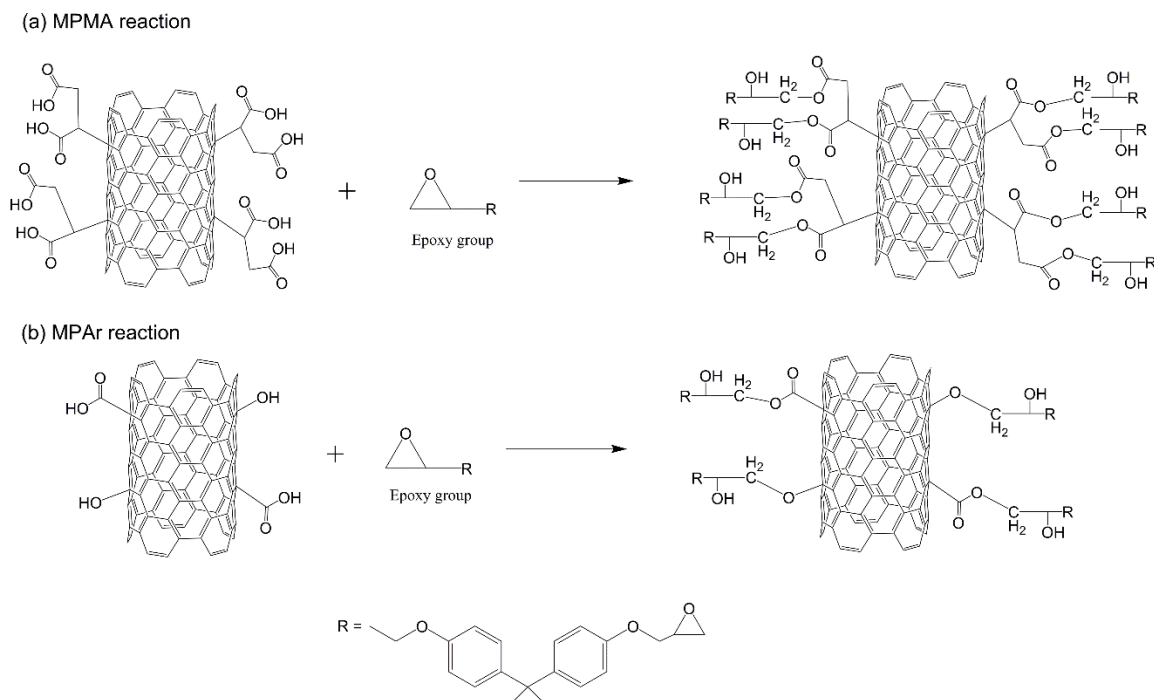


Figure 4.8: (a) MPMA and (b) MPAR reactions with epoxy groups leading to enhancement of interfacial interactions between the fiber and the matrix.

The interface strength was measured by the shear stress between the fiber-matrix through the utilization of a microbond technique.¹³ This technique measured the interfacial shear stress of a single fiber that was embedded in an epoxy microbead. It was assumed that debonding occurred at the critical force applied, it would de-bond throughout the entire embedded length. The embedded length was kept between 0.05 mm to 1.0 mm to reduce the chance of pre-mature fiber fracture. Dimensions of the epoxy bead embedded fiber and fiber diameter was measured by using a Leica DM2500M microscope with magnifications of x5 and x20, shown in Figure 4.9.

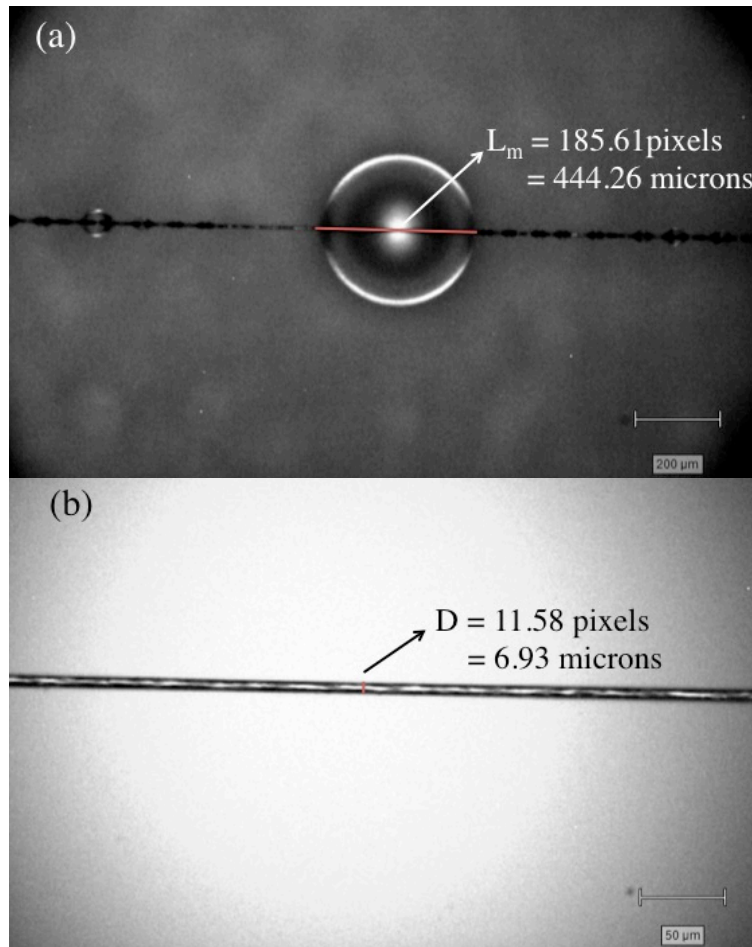


Figure 4.9: Microbond images (a) epoxy microbead (l_m) (b) fiber diameter (d).

After the single fiber was mounted into the apparatus, as shown in Section 3.4.3 Figure 3.5, a force was applied to induce shear affects at the fiber-matrix interface until debonding occurred. This experiment was repeated to obtain a statistical average (minimum of 30 data points) for PAN-based, MPMA, and MPAr interfacial shear stress measurements. The summary of the results is presented in Table 4.2.

Table 4.2: Interfacial shear stress values from microbond technique.

	Embedded length (μm)	Diameter of fiber (μm)	Interfacial shear stress (MPa)	Relative percent difference (%)
PAN-based	398.82 ± 16.98	6.88 ± 0.22	13.06 ± 1.71	---
MPMA	395.97 ± 16.31	7.01 ± 0.25	13.93 ± 1.75	6.70
MPAr	373.98 ± 19.66	7.00 ± 0.24	12.99 ± 1.87	0.53

The MPMA enhanced surfaces indicated an increase in the interfacial shear stress within error. This indicates that the functional groups reacted with the epoxy groups to create a stronger interface between the two phases, illustrated in Figure 4.8a. The MPAr enhanced surfaces showed that the interfacial shear stress did not improve compared to PAN-based carbon fiber surfaces. The MPAr was expected to react with the epoxy groups illustrated in Figure 4.8b. As discussed in Section 4.1.3, the mechanism behind the MPAr reaction is based on plasma etching the surface of the fiber of contaminants and generated functional groups that formed due to free radicals reacting with air.¹⁰ In other studies that utilized Ar gas as a plasma to enhance the fiber-matrix interface, it is mentioned that argon gas surface modifications did not enhance the interfacial shear stress even though there was appearances of functional groups. Another reason why argon gas plasma did not enhance

the interfacial fiber-matrix is because the modification focuses on altering the physical surface morphology by making the surface more porous.^{11,14}

4.3 CORRELATION OF SPECTROSCOPIC AND MECHANICAL ANALYSIS

In Section 4.1, the MPSM focused on characterization of the surfaces of the reacted carbon fibers. To summarize the changes, hybridization of the surface from sp^2 to sp^3 was observed by Raman spectroscopy. Furthermore, ATR-FTIR spectroscopy revealed the formation of -COOH and -OH functional groups are formed by MPMA and MPAr reactions. Microbond measurements described, in Section 4.2, showed how the MPSM would enhance the fiber-matrix interface through shear stress. The characterization of the surface and interfacial shear stress measurements can be correlated to predict the outcome. To illustrate the correlation between fiber surface characterization and fiber-matrix interactions, Table 4.3 summarizes the I_D/I_G Ratio measured in Raman spectroscopy and the corresponding interfacial shear stress measured by the microbond technique. Raman spectroscopy was used to monitor the hybridization change from sp^2 to sp^3 conformations on the surface of the carbon fibers. As the I_D/I_G Ratio changed it can be correlated and observed in changes that occurred in the shear stress measurements. The PAN-based I_D/I_G Ratio was 1.36 ± 0.23 that had a shear stress of 13.06 ± 1.71 MPa. As the carbon fibers were treated with MPMA, the I_D/I_G Ratio increased to 1.99 ± 0.19 while the shear stress indicated an increase to 13.93 ± 1.75 MPa within error. Carbon fibers treated with MPAr, the I_D/I_G Ratio was 1.30 ± 0.19 which was similar to the PAN-based ratio and exhibited a similar shear stress.

Table 4.3: Summary of interfacial shear stress values and I_D/I_G ratio.

	I_D/I_G ratio	Interfacial shear stress (MPa)
PAN-based	1.36 ± 0.23	13.06 ± 1.71
MPMA	1.99 ± 0.19	13.93 ± 1.75
MPAr	1.30 ± 0.19	12.99 ± 1.87

Table 4.3 is visually represented in Figure 4.10 to show how the I_D/I_G Ratio can be correlated to interfacial shear stress to predict how MPSM affect the surface of carbon fiber surfaces.

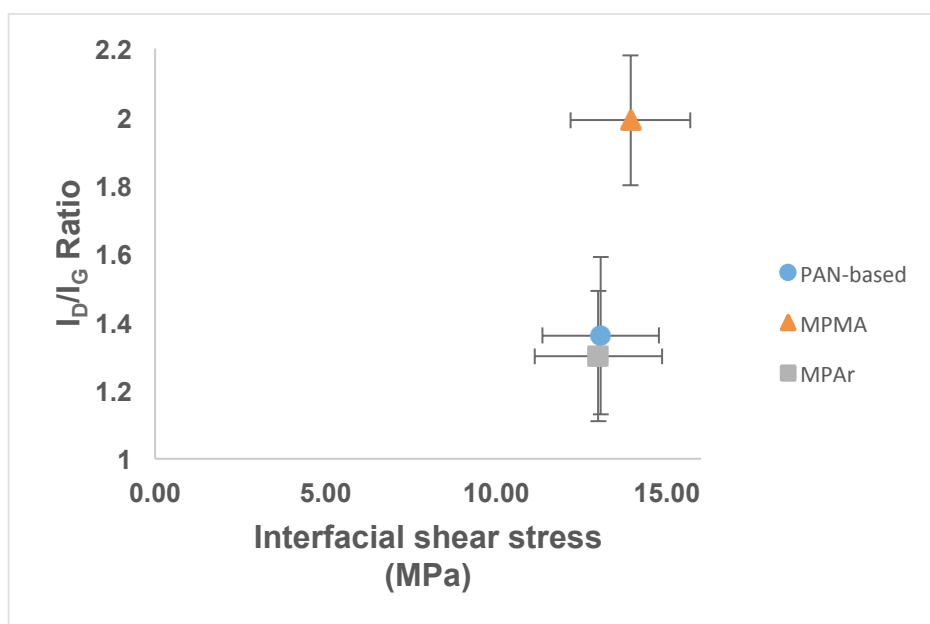


Figure 4.10: I_D/I_G ratios plotted as a function versus interfacial shear stress (MPa) for PAN-based, MPMA, and MPAr.

Understanding how interfacial shear stress is related to analytical techniques is important because it will enable predications of MPSM. Using Raman spectroscopy semi-quantitatively analyze the extent of changes on the carbon fiber surfaces was determined.

4.4 SUMMARY AND CORRELATION TO COMPOSITE MECHANICAL PROPERTIES

In an effort to relate the above results to practical applications in composites, we estimated how surface modifications will impact the composite tensile strength. In Section 4.2 the shear stress quantified the modified surfaces of carbon fibers. This interfacial shear stress acts as an opposing force to the force being applied to the composite. Figure 4.10 demonstrates how the difference of an unmodified and modified carbon fiber would appear in a composite. Figure 4.11a shows that the epoxy matrix will de-bond from the carbon fiber after a force is applied. Figure 4.11b shows that the epoxy matrix has taken a higher force to de-bond from a modified carbon fiber surface, such as MPMA.

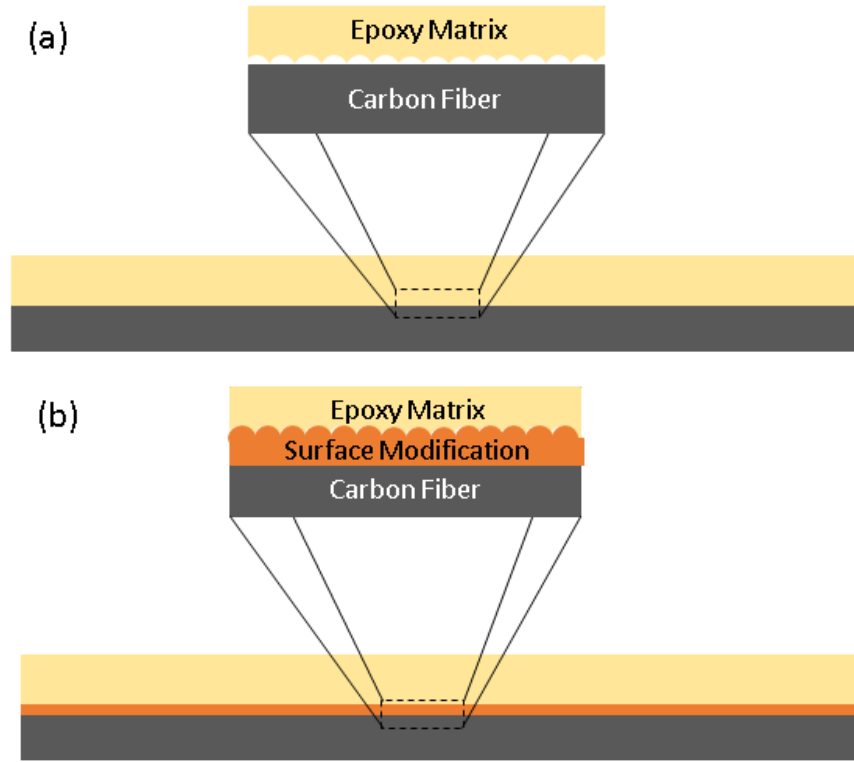


Figure 4.11: Schematic diagram of interfacial interfaces of (a) unmodified and (b) surface modified carbon fiber surfaces.

Utilizing the interfacial shear stress equation (Eqn. 3.1) can be correlated to predicting the tensile strength in a composite. The Rule of Mixtures (Eqn. 4.1) estimates the composite tensile strength (σ_c^*) utilizing the fiber tensile strength (σ_f^*) and matrix tensile strength (σ_m^*). The Rule of Mixtures takes in consideration the volume fraction of each component in the system, shown in Eqn. 4.1.¹⁵

$$\sigma_c^* = \sigma_f^* v_f + \sigma_m^* (1 - v_f) \quad (4.1)$$

This calculated prediction takes in account the interfacial shear stresses through the critical length (l_c) of the composite and predicts how the composite will fail. The critical

length is calculated, using Eqn. 4.2, using the tensile strength of the fiber (σ_f^*) and the diameter (d) over the interfacial shear stress (τ_i).¹⁵

$$\frac{l_c}{d} = \frac{\sigma_f^*}{4\tau_i} \equiv l_c = \frac{\sigma_f^* d}{4\tau_i} \quad (4.2)$$

If the length of the composite is less than the critical length, then the failure will occur at the interface between the carbon fiber surfaces and the matrix material. If the length of the composite is greater than the critical length, then the fiber will fail. In our composite, the length of the composite is greater than the critical length, so the failure will occur due to the fiber failing. Failure in the fiber, Eqn. 4.1 was modified to incorporate the critical length (Eqn. 4.2) to produce the Eqn. 4.3.¹⁵

$$\sigma_c^* = \sigma_f^* \left(1 - \frac{l_c}{2l}\right) v_f \eta + \sigma_m' (1 - v_f) \quad (4.3)$$

The strength of the fiber (σ_f^*) incorporates the interfacial shear stress through the critical length (l_c). The critical length is incorporated into the equation because it assumes that the load will be the same in the fiber and matrix. The assumptions for using Eqn. 4.3 are the following: a composite fiber length of 1 cm, matrix tensile strength is 0.100 GPa, fiber orientation efficiency is 1, fiber volume fraction is 0.60, and applied force in the longitudinal direction. The τ_i and d values are from the data collected for Section 4.2. The predicted composite tensile strength and critical length are displayed in Table 4.4. shown as PAN-based, MPMA, and MPAr reactions.

Table 4.4: Estimations of critical length and composite tensile strength.

	Critical length (l_c)	Estimated Composite Tensile Strength (GPa)	Relative Percent Difference (%)
PAN-based	0.073 ± 0.020	2.372 ± 0.025	---
MPMA	0.065 ± 0.016	2.382 ± 0.020	0.43
MPAr	0.070 ± 0.017	2.376 ± 0.020	0.15

Failure in the fiber, the estimated tensile strength shows that there is an indication of increase of approximately 10 MPa in the MPMA reaction compared to the PAN-based.

The tensile strength in the MPAr reaction had approximately 40 MPa compared to PAN-based. Table 4.5 summarizes the interfacial shear stress of the modified carbon fiber surfaces to the estimated composite tensile strength both the two conditions, and plotted is in Figure 4.12.

Table 4.5: The summary shear stress and estimated composite tensile strength values.

	Interfacial shear stress (GPa)	Estimated composite tensile strength (GPa)
PAN-based	0.0131 ± 0.00171	2.372 ± 0.025
MPMA	0.0139 ± 0.00175	2.382 ± 0.020
MPAr	0.0129 ± 0.00187	2.376 ± 0.020

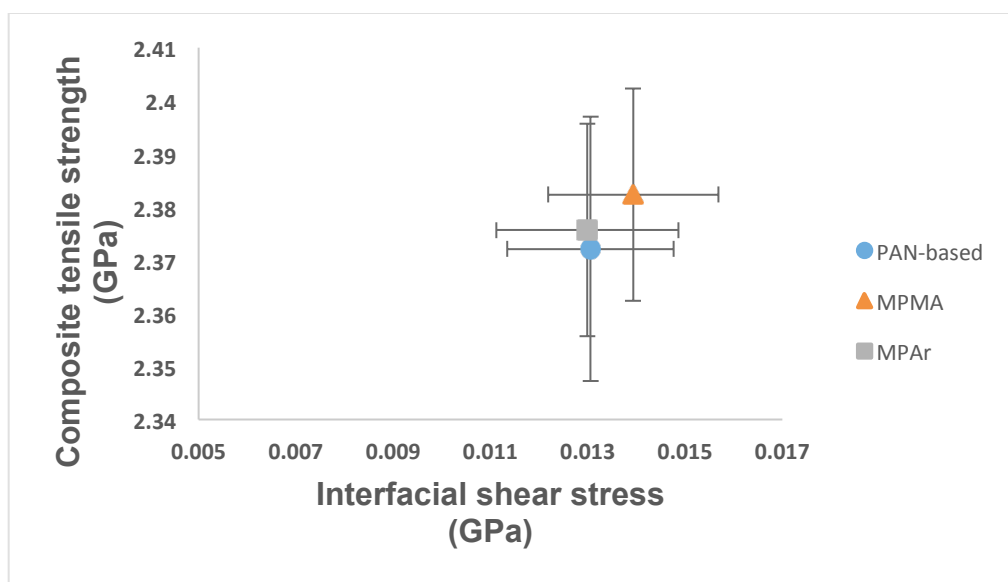


Figure 4.12: Estimated composite tensile strength (GPa) plotted as a function versus interfacial shear stress (MPa) failure in the fiber for PAN-based, MPMA, and MPAr.

4.5 SUMMARY AND FUTURE WORK

These studies illustrated that solventless carbon fiber surface modifications can be effectively employed in order to achieve enhanced fiber-matrix mechanical properties. This was achieved by the use of microwave plasma, which generated acid groups on the surface of carbon fibers, thus facilitating covalent bonding between the fiber and an epoxy matrix. Using shear stress analysis to evaluate mechanical properties combined with spectroscopic analysis these studies showed that the predicted composite mechanical properties were enhanced in MPMA. The MPMA reactions showed enhanced properties by 6.08 % with failure at the interface and 0.43 % with failure occurring in the fiber. Future work will include the development and testing of continuous fiber processing which can be utilized in surface modification of many fibers.

REFERENCES

1. Y. Zhao, Y.; Urban, M.W., Spectroscopic studies of microwave plasma reactions of maleic anhydride on poly(vinylidene fluoride) surfaces: crystallinity and surface reactions. *Langmuir*, **1999**, *15*(10), 3538-3544.
2. McMurry, J.E. *Organic Chemistry*. Brooks Cole: Boston, **2012**.
3. Sadezky, A.; Muckenhuber, H.; Niessner, R.; Poschl, U., Raman microspectroscopy of soot and related carbonaceous materials: spectral analysis and structural information. *Carbon*, **2005**, *43*(8), 1731-1742.
4. Aumsuwan, N.; Ye, S.H.; Wagner, R.; Urban, M.W., Covalent attachment of multilayers on Poly(tetrafluoroethylene) surfaces. *Langmuir*, **2011**, *27*(17), 11106-11110.
5. Pearson, H.A.; Urban, M.W., Simple click reactions on polymer surfaces leading to antimicrobial behavior. *J. Mater. Chem. B*, **2014**, *2*(15), 2084-2087.
6. Dandekar, A.; Baker, R. T. K.; Vannice, M. A., Characterization of activated carbon, graphitized carbon fibers and synthetic diamond powder using TPD and DRIFTS. *Carbon*, **1998**, *36*(12), 1821-1831.
7. Fanning, P. E.; Vannice, M. A., A DRIFTS study of the formation of surface groups on carbon by oxidation. *Carbon*, **1993**, *31*(5), 721-730.
8. Socrates, G. *Infrared and Raman characteristic group frequencies: tables and charts*. John Wiley & Sons: Chichester, **2004**.
9. Yuan, L.Y.; Shyu, S.S.; Lai, J.Y., Plasma surface treatments of carbon fibers. Part 2: Interfacial adhesion with poly(phenylene sulfide). *Composites science and technology*, **1992**, *45*(1), 9-16.

10. Donnet, J.B.; Dhami, T.L.; Dong, S.; Brendle, M., Microwave plasma treatment effect on the surface energy of carbon fibres. *Journal of Physics D: Applied Physics*, **1987**, 20(3), 269-275.
11. Jang, B.Z., Control of interfacial adhesion in continuous carbon and Kevlar fiber reinforced polymer composites. *Composites science and technology*, **1992**, 44(4), 333-349.
12. Coburn, J.W.; Winters, H.F., Plasma etching – A discussion of mechanisms. *Journal of Vacuum Science & Technology*, **1979**, 16(2), 391-403.
13. Herrera-Franco, P.J.; Drzal, L.T., Comparison of methods for the measurement of fibre/matrix adhesion in composites. *Composites*, **1992**, 23(1), 2-27.
14. Li, R.; Ye, L.; Mai, Y.W., Application of plasma technologies in fibre-reinforced polymer composites: a review of recent developments. *Composites Part A: Applied Science and Manufacturing*, **1997**, 28(1), 73-86.
15. Chawla, K.K., *Composite materials: Science and Engineering*. Springer Science & Business Media: New York, **2012**.

CHAPTER FIVE

CONCLUSION

The main objective of this research was to investigate the effects of microwave plasma surface modifications on enhancing the interfacial relationship between the fiber and the matrix (epoxy). The interfacial relationship is critical because it affects how the load is distributed throughout the composite material. Carbon fibers were studied because of the versatility of carbon fiber reinforced plastic composites; however, they have an inherent problem of having an inert fiber surface. This inertness makes it difficult for the matrix to interact and create a strong adhesive bond between the two phases. One of the solutions to solve this inert surface is to subject the fiber surfaces to chemical surface modifications that would generate functional groups. Microwave plasma surface modifications were utilized to functionalize the surface of carbon fibers -COOH and -OH groups. This was accomplished by treating the surface with MA monomer and Ar gas. The results of the experiments performed were utilized to develop an understanding of how the surface was affected through ATR-FTIR spectroscopy, Raman spectroscopy and mechanical properties at the interface. The ATR-FTIR monitored the formation of -COOH and -OH functional groups, and distinguishes the difference between the MPMA and MPAr reactions. The ATR-FTIR results showed that the microwave plasma cleaved the C=C bond on the carbon fiber surface to generate free radicals during the process. MPMA reaction showed that the C=C bond in the monomer was cleaved and attached itself to the surface to form the functional groups. The MPAr reaction etched the surface

to generate the functional groups. Raman spectroscopy was utilized to compliment the ATR-FTIR results in order to develop the mechanism by monitoring the changes in the I_D/I_G ratio. The ratio was related to the sp^2 and sp^3 hybridization present on the carbon fiber surface. The I_D/I_G ratio in the MPMA reaction increased compared to PAN-based. The I_D/I_G ratio in the MPAr reaction was similar to the I_D/I_G ratio of PAN-based. These results lead to the development of a possible mechanism for MPMA and MPAr reactions described in Section 4.1.3. The enhance interface between the modified carbon fiber surfaces and an epoxy matrix was monitored by a microbond technique that measured the interfacial shear stress. The interfacial shear stress results showed that the MPMA reaction had improved adhesion due to the functional groups formed at the interface. The MPAr reaction had similar interfacial shear stress results compared to the PAN-based because the functional groups generated in this method did not improve the fiber-matrix relationship. The interfacial shear stress measurements and Raman spectroscopy were used to establish a relationship that could predict the shear stress by the hybridization changes on the modified surfaces. To complete the objective of the research, the results of the surface modifications were related to practical applications through predicting the composite tensile strength. This was predicted through interfacial shear stress where failure would occur at the interface of the composite. The overall composite was predicted to have a better interface between the fiber and the matrix through MPMA surface modifications. The research demonstrated that microwave plasma surface modification is a viable method to treat fiber materials for composite materials to

enhance the interfacial relationship of the fiber-matrix. This process was fast, efficient, solvent less, and promoted chemical reactions on the substrate material.